

Prepared for:

MARSHALL SPACE FLIGHT CENTER, AL 35812  
GEORGE C. MARSHALL SPACE FLIGHT CENTER

(NASA-CR-184068) LASER ATMOSPHERIC WIND  
SOUNDER (LAMS) PHASE 1 • VOLUME 1: EXECUTIVE  
SUMMARY FINAL REPORT, 24 Mar. 1989 - 23 Mar.  
1990 (LMSC) 71 p. CSC 148

63135 Unclassified  
0325632

NO1-17351



LMSC-HSV T8 40220203

CR-184068

DR-19  
**Final Study Report (Phase I)**  
for  
**Laser Atmospheric Wind Sounder  
(LAWS)**

**Volume I Executive Summary**

Submitted in Partial Fulfillment of

Contract NAS8-37590

April 1990

Prepared for:

**GEORGE C. MARSHALL SPACE FLIGHT CENTER  
MARSHALL SPACE FLIGHT CENTER, AL 35812**

Submitted by:

  
**Lockheed**  
*Missiles & Space Company, Inc.*

4800 Bradford Blvd., Huntsville, AL 35807

  
\_\_\_\_\_  
W.E. Jones, Project Manager  
LAWS Project Office  
Lockheed - Huntsville

## FOREWORD

This document presents the final results of the 12-month Phase I effort for the Laser Atmospheric Wind Sounder (LAWS). This work was performed for the Marshall Space Flight Center (MSFC) by Lockheed Missiles & Space Company, Inc., Huntsville Engineering Center, under Contract NAS8-37590. The study was conducted under the direction of R.G. Beranek, NASA Program Manager, PS02. Period of performance was 24 March 1989 to 23 March 1990.

The complete Phase I Final Report consists of the following three volumes:

- Volume I - Executive Summary
- Volume II - Final Report
- Volume III - Program Cost Estimates.

Subcontractors contributing to this effort are Avco Research Laboratory, Inc.; GEC Avionics Ltd.; and Itek Optical Systems.

TABLE OF CONTENTS

<u>Section</u>	<u>Page</u>
FOREWORD.....	ii
TABLE OF CONTENTS.....	iii
LIST OF ILLUSTRATIONS.....	iv
LIST OF TABLES.....	v
1 LAWS CONCEPT INTRODUCTION.....	1
2 LAWS SUBSYSTEM DESIGNS.....	6
2.1 Optical Subsystem.....	6
2.2 Laser Subsystem.....	12
2.2.1 Avco Research Laboratory (ARL) Transmitter Configuration.....	13
2.2.2 GEC Avionics (GEC) Transmitter Configuration...	19
2.3 Receiver/Processor Subsystem Summary.....	27
2.4 Command, Communication, and Control Subsystem.....	31
2.5 Electrical Power Subsystem.....	35
2.6 Mechanical Support Subsystem.....	38
3 PERFORMANCE ANALYSIS.....	40
4 LAWS BASELINE CONFIGURATION AND ACCOMMODATION.....	47
4.1 Alternate LAWS Configuration.....	52
5 PROJECT COST ESTIMATES.....	57
5.1 Cost Estimating Methodology.....	57
5.2 LAWS Project WBS Elements.....	58
5.3 Summary Cost Presentations.....	63
5.4 Funding Profiles and Expenditures Data.....	64

LIST OF ILLUSTRATIONS

<u>Figure</u>		<u>Page</u>
1	Lockheed Design Enhances LAWS System Requirements.....	2
2	LAWS Top-Level Functional Diagram.....	3
3	LAWS System Diagram.....	4
4	LAWS Instrument Packaging.....	5
5	Optical Subsystem Requirements/Specifications.....	7
6	Optical Subsystem Efficiency Budget.....	9
7	LAWS Telescope Configuration.....	10
8	Optical Bench Assembly .....	11
9	Gimbal Assembly.....	11
10	Transmitter Laser Requirements.....	13
11	Schematic of the Injection Locking Method.....	14
12	AVCO Laser Baseline Design.....	17
13	Baseline Avco Design Power/Efficiency for 20 J/pulse, 8 Hz Transmitter.....	20
14	Avco Laser Head Concept.....	21
15	LAWS Laser Subsystem Block Diagram.....	30
16	LAWS Laser Subsystem Modular Arrangement.....	30
17	LAWS Laser Subsystem External View.....	31
18	GEC Laser Head Concept.....	32
19	System Power and Weight Summary.....	33
20	LAWS Receiver/Processor Block Diagram.....	34
21	LAWS Flight Data Management Functional Hierarchy.....	35
22	LAWS Software Tree.....	36
23	LAWS Flight Software Command and Data Flow Management .....	37
24	Electrical Parameters as Function of Position in POP Orbit for Typical 100 Minute Orbit.....	39
25	Optimal Allocation of Power for 20 J Maximum Laser Pulse Energy (Cramer-Rao Estimator).....	41
26	Optimal Allocation of Weight for a 400 kg Sum of Laser Mass and Telescope Mass.....	41
27	400 kg Combined Laser/Telescope/Motor/Bearing Concept Trades...	42
28	Trade of Global Coverage vs Data Quality as Expressed by SNR for Low Backscatter (High Altitude).....	43
29	Azimuth Controlled Pulsing.....	43
30	Scanning and Latitude Shot Management.....	44
31	Short Pulse (1.6 $\mu$ sec) and Window Lengths of 32 (Matched), 64 (x2), and 128 (x4) Samples (Wind field with velocity gradient reversals every 1 km).....	45
32	Short Pulse (1.6 $\mu$ sec) and Window Lengths of 32 (Matched), 64 (x2), and 128 (x4) (Continuously varying wind field).....	46
33	LAWS Baseline Configurations.....	48
34	Typical LAWS/POP Configuration.....	48

LIST OF ILLUSTRATIONS (Concluded)

<u>Figure</u>		<u>Page</u>
35	LAWS with Radiator.....	50
36	Space Station Installation.....	50
37	Shuttle Launch Configuration.....	51
38	H-II Launch Configuration.....	51
39	Preliminary JPOP/LAWS.....	53
40	Alternate LAWS Configuration.....	53
41	JPOP Installation.....	54
42	H-II Launch Configuration.....	54
43	Space Station Installation.....	55
44	Shuttle Launch Configuration.....	55
45	LAWS Project Work Breakdown Structure.....	59
46	Preliminary LAWS Master Schedule for JPOP Phase C/D.....	61
47	LAWS Instrument Cost Elements.....	62
48	JPOP and Space Station Development Cost.....	64
49	Projected Funding Profiles for LAWS Phase C/D to Develop the JPOP Configuration.....	65

LIST OF TABLES

<u>Table</u>		<u>Page</u>
1	GEC Laser Subsystem Design Guidelines.....	28
2	LAWS Baseline Parameters.....	49
3	Baseline Configuration/GEC Laser.....	49
4	Alternate Configuration/Avco Laser.....	56

## SECTION 1. LAWS CONCEPT INTRODUCTION

The Laser Atmospheric Wind Sounder (LAWS) will provide a new space based capability for the direct measurement of atmospheric winds in the troposphere. LAWS will make a major contribution toward advancing our understanding and prediction of the total earth system and NASA's Earth Observing System (EOS) program. LAWS is designed to measure a fundamental atmospheric parameter required to advance weather forecasting accuracies and investigate global climatic change. LAWS has a potential added benefit of providing (global) concentration profiles of large aerosols including visible and subvisible cirrus clouds, volcanic dust, smoke, and other pollutants.

The objective of this Phase I study - to develop a LAWS concept and configuration - is met through the instrument design outlined in this Executive Summary, and depicted in more detail in Volume II. Highpoints of the Lockheed LAWS instrument design are shown in Figure 1 as they relate to the top-level, NASA-suggested requirements and specifications.

Figure 1 relates the specifications of the NASA Strawman LAWS System to the Lockheed system design and discusses how these design parameters meet or exceed LAWS requirements. All LAWS Instrument design specifications have been chosen to assure a performance level meeting or exceeding the Strawman performance requirements presented by NASA in the Statement of Work (SOW). In the case of the laser pulse, we are considering pulse lengths equal to or shorter than the Strawman (3  $\mu$ sec) pulse length to enhance range resolution, provide a correlation time consistent with atmospheric turbulence decorrelation, and allow for additional independent samples along each laser shot. Pulsing the laser upon demand rather than at a fixed repetition rate is a design feature which conserves laser (and overall instrument) power, leads to longer operational lifetime, and allows optimal selection of datum locations.

Increasing the laser energy from 10 to 20 J/pulse doubles the system sensitivity and provides more accurate measurements in global regions of lower aerosol concentrations. Increasing the transmitter/receiver aperture from 1.5 to 1.67 m through the use of our larger telescope primary mirror provides an additional 20 percent improvement in system sensitivity. Also, a selectable off-nadir scan angle allows optimization of scan angle for global coverage versus system sensitivity since the global backscatter profiles (to which this parameter is optimized) will not be well defined until measured by LAWS. These concept features have been selected with cost reality as a major driver.

In developing the LAWS concept/configuration, Lockheed initially examined functional requirements for LAWS. These are depicted at the top level in the functional diagram of Figure 2. From this functional analysis and flow-down,

NASA Strawman LAWS System	Lockheed LAWS System
<b>Coherent Lidar</b> <ul style="list-style-type: none"> <li>Pulsed Transmitter (<math>\text{CO}_2</math>)</li> <li><math>9.11 \mu\text{m}</math> Wavelength</li> <li>• 3 <math>\mu\text{sec}</math> Pulse Length</li> <li>• 10 Hz PRF</li> <li>• 10 Joules/Pulse</li> <li>• 5% Wallplug Efficiency</li> <li>• <math>10^9</math> Shots Lifetime</li> </ul>	<b>Coherent Lidar</b> <ul style="list-style-type: none"> <li>Pulsed Transmitter (<math>\text{CO}_2</math>)</li> <li><math>9.11 \mu\text{m}</math> Wavelength (<math>11.2 \mu\text{m}</math> being Considered) A</li> <li>• 1 <math>\mu\text{sec}</math> - 3 <math>\mu\text{sec}</math> B</li> <li>• 1 - 10 Hz on Demand C</li> <li>• 20 Joules/Pulse D</li> <li>• 5% Wallplug Efficiency</li> <li>• <math>10^9</math> Shots Lifetime</li> </ul>
<b>Telescope</b> <ul style="list-style-type: none"> <li>• 1.5 m Aperture</li> <li>• 6 rpm Scan Rate</li> <li>• 45 deg Nadir Angle</li> </ul>	<b>Telescope</b> <ul style="list-style-type: none"> <li>• 1.67 m Aperture E</li> <li>• 6.6 rpm F</li> <li>• 35, 45, 55 deg G Nadir Angles</li> </ul>

LAWS - 10

NASA Strawman Requirements	Lockheed Design Meets or Exceeds Requirements	Specification Impact
• Global Wind Measurements commensurate with coverage	With variable scan angle, can adjust scan in orbit for optimal coverage and sensitivity	G
• Horizontal Resolution of $100 \times 100 \text{ km}$	With pulse upon demand, can adjust laser firing for optimal coverage	C
	6.7 rpm provides approx. 1.5 pulses per 100 km swath as satellite passes over	F
• Vertical Resolution of 1 km	1 to 3 $\mu\text{sec}$ pulse provides a vertical resolution of approx. 200 to 600 m. Pulse length to be refined during Phase II.	B
• Horizontal Wind Vector $\pm 1 \text{ m/s}$ in lower and $\pm 5 \text{ m/s}$ in upper troposphere	A function of pulse length, atmospheric decorrelation and system sensitivity. 1 to 3 $\mu\text{sec}$ pulse length is commensurate with velocity accuracy requirement. Higher energy (20 J) and larger aperture (1.67 m) enhances sensitivity and therefore accuracy.	A D E
• Operational Lifetime of $10^9$ shots	Meets requirements. Fire upon demand extends operational lifetime in years on orbit by judicious placement of shots.	C
• Serviceability	Meets requirements. Takes advantage of HST derived experience. Likely not required for JPOP.	
• 800 kg wt budget	Meets requirement.	
• 3 kW power budget	Operates with 2.5 kW average power from 800 km orbit or 2 kW from 705 km orbit.	D C G E
• Shot mgmt to optimize Distribut. Pattern	Fire upon demand provides optimal shot management.	C
• $\beta = 10^{-11} \text{ to } 10^{-7} / \text{m SR}$	Larger aperture, higher energy enhances sensitivity to lower values of $\beta$ .	A E

LAWS-11

Figure 1. Lockheed Design Enhances LAWS System Requirements

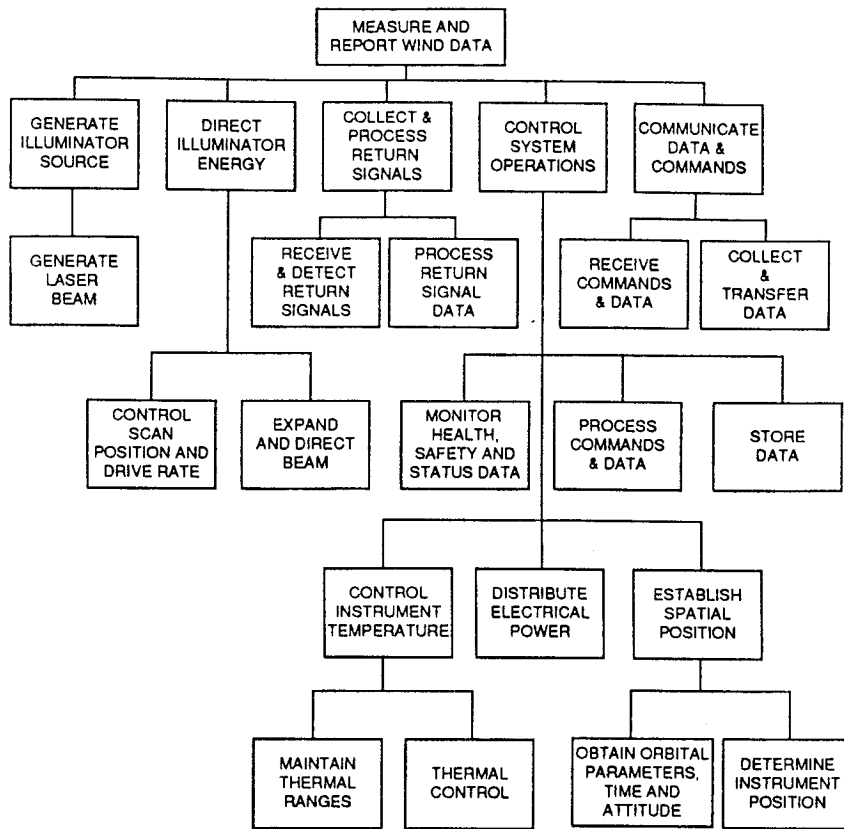


Figure 2. LAWS Top-Level Functional Diagram

LAWS system was synthesized as depicted in Figure 3. The LAWS Instrument functions are performed by the six subsystems of Figure 3: laser; optical; receiver/processor; command control, and communications; mechanical support; and electrical power. Figure 3 depicts in simplified form some of the interfaces between these subsystems and several of the major assemblies within the subsystems. These subsystems are further outlined in the sections of this executive summary which follow.

Figure 4-A depicts the LAWS configuration packaged for launch in the Japanese H-II launch vehicle for deployment as an instrument of the Japanese Polar Orbiting Platform (JPOP). Figure 4-B depicts LAWS mounted on JPOP with its radiator deployed for instrument thermal control. Figure 4-C illustrates LAWS subsystems and assemblies mounted upon a base structure for kinematic attachment to JPOP or Space Station Freedom (SSF). Attachment to SSF via the payload interface adapter is depicted in Figure 4-D. Definitive interfaces with JPOP and SSF will be developed as the designs of these platforms mature. The Lockheed LAWS Instrument configuration weight is less than the 800 kg allocated by NASA. Average power requirements are also considerably less than the 3 kw specified in the Phase I SOW.

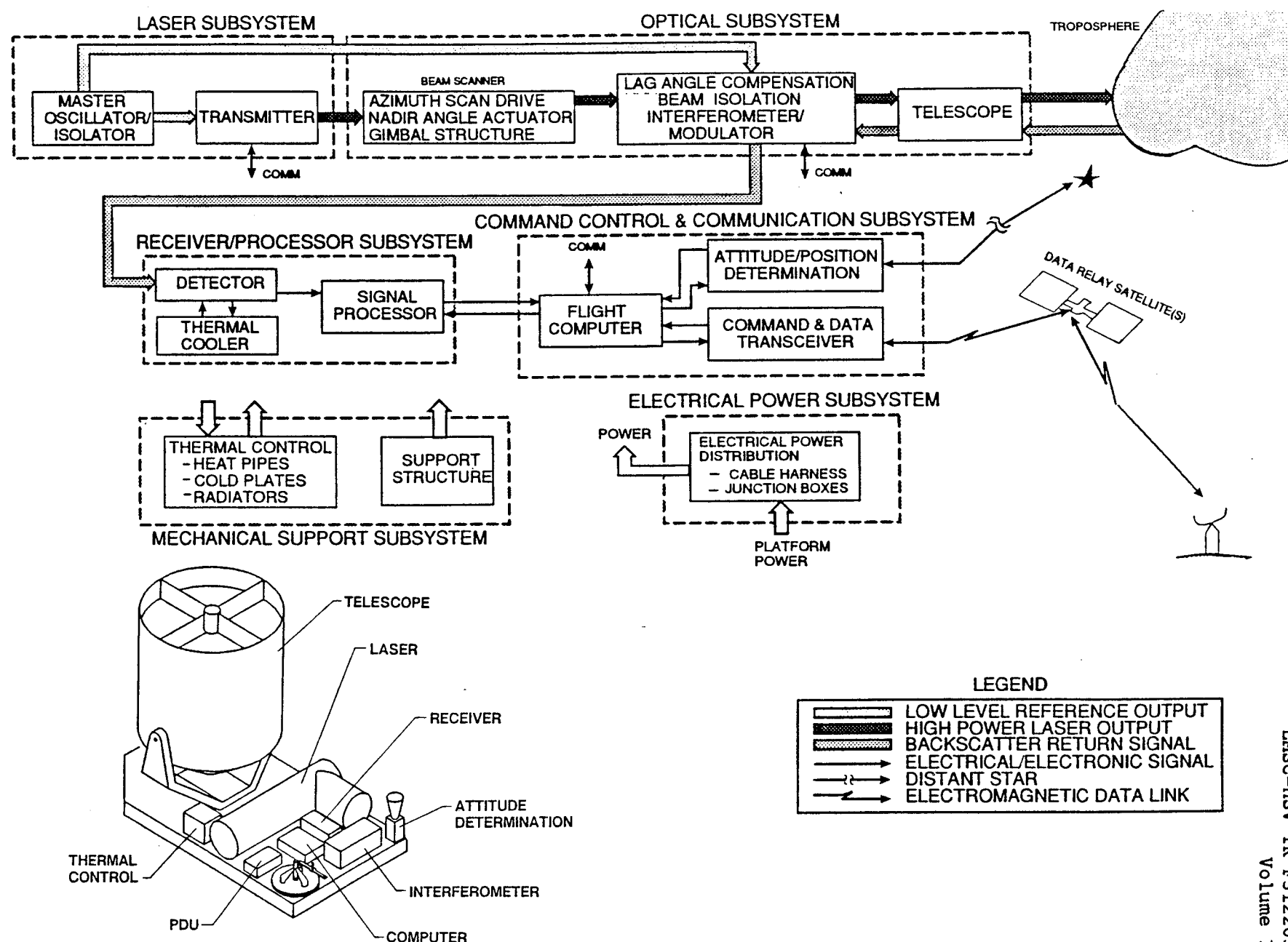
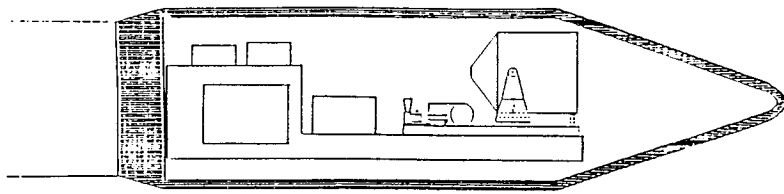
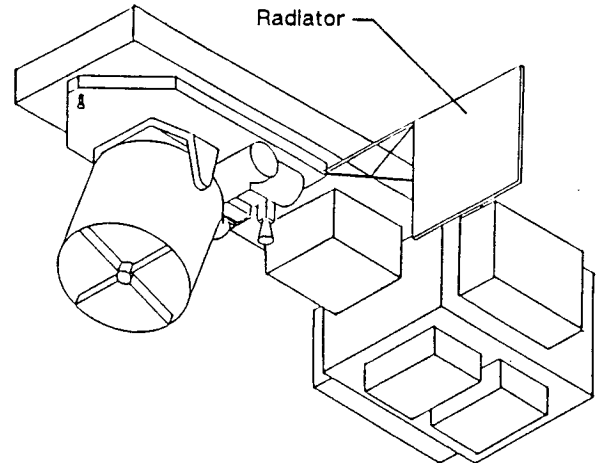


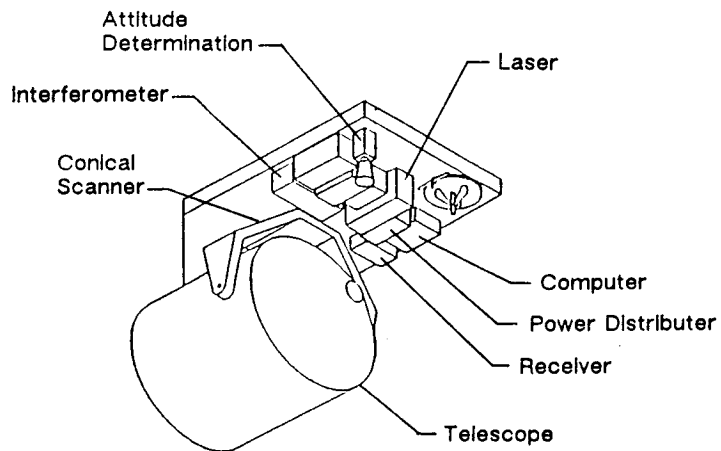
Figure 3. LAWS System Diagram



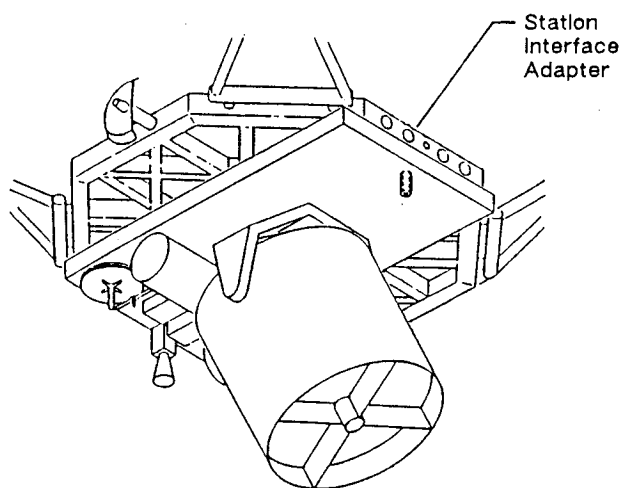
(a) LAWS Packaged for  
H-II Launch



(b) Suggested JPOP Configuration  
of LAWS Instrument



(c) LAWS Hardware Packaging  
(GEC Laser Depicted)



(d) Space Station Installation  
(AVCO Laser Depicted)

Figure 4. LAWS Instrument Packaging

## SECTION 2. LAWS SUBSYSTEM DESIGNS

This section describes the LAWS subsystems beginning with the Optical Subsystem (2.1) and continuing through the Laser (2.2), Receiver/Processor (2.3), Communications, Command, and Control (2.4), Electrical Power (2.5), and Mechanical Support (2.6).

### 2.1 OPTICAL SUBSYSTEM

As the LAWS platform orbits the earth, the Optical Subsystem points the telescope off of nadir and then rotates the whole telescope about the nadir axis, producing a conical scan. Scanning at substantial angular rates coupled with large slant ranges causes the return beam to lag behind the telescope by up to 8 mrad. This lag angle must be compensated in real time to a precision of less than 1.5  $\mu$ rad. The 1.5  $\mu$ rad requirement comes about because of the necessity to align the wavefronts of the return beam and the local oscillator in order to maximize the heterodyne detection efficiency.

The LAWS Optical Subsystem fundamentally operates in two modes, transmit and receive. While in the transmit mode, the optical system couples a pulsed laser to a telescope which transmits the beam approximately 1200 km to the earth's atmosphere which then scatters portions of the energy. Some of this radiation is scattered back in the direction of the transmitted pulse and is collected by the LAWS Optical Subsystem, which has been switched into its receive mode. In this mode, the telescope collects the backscattered radiation which the interferometer combines with local oscillator laser radiation as both are directed into the heterodyne receiver.

The LAWS Optical Subsystem meets all the specified performance requirements and all the derived requirements described throughout this report. The system achieves this using low risk technologies, providing confidence in producibility and space operations.

The LAWS Optical Subsystem concept was developed by Itek Optical Systems, a Division of Litton Industries, as a subcontractor to Lockheed Missiles & Space Co., with assistance from Laser Systems & Research and Northeastern University, two Lockheed consulting groups.

Optics Requirements. The top level LAWS optical system requirements, shown in Figure 5(a), were used to determine the specifications of Figure 5(b). The first of these specifications is a result of the need to couple the collimated transmitter laser output into the atmosphere approximately 1200 km away. Because of the great distance to the target, an afocal beam expander is required. With a 4 cm x 4 cm transmitter laser output and a 1.67 m diameter telescope (for S/N considerations) the required system (beam expander) magnification is 42X.

● Weight	$\leq 225 \text{ kg}$
● Diameter	$\geq 1.67 \text{ m}$
● Lag Angle Compensation @ 6.8 rpm	$35^\circ, 45^\circ, \text{ and } 55^\circ$ cone half angles and $705 - 800 \text{ km orbits}$
● Pointing Accuracy	$\leq 3 \mu\text{rad} (2\sigma)$
● Variable Off Nadir Scan Angle	$35^\circ \leq x \leq 55^\circ$
● Size Compatible with JPOP and Shuttle	

(a) LAWS Optical Subsystem Requirements

● Afocal Telescope	
● Full Field of View	$1^\circ$
● Wavelength	$9.11 \mu\text{m}$
● Magnification	$\sim 42X$
● Performance ( $g = 9.11 \text{ m}$ )	$0.07 \text{ \AA rms}$
● Obscuration	< 7% area
● Accessible Pupil	Low Distortion

(b) Flow-Down Specifications

Figure 5. Optical Subsystem Requirements/Specifications

The second of the flow-down optics specifications results from the lag angle created by the conical scanning pattern. For the baseline 6.8 rpm rotation rate and the maximum nadir angle of 60°, a full field of view of 16 mrad ( $\sim 1.0$  deg) is necessary.

The requirement for an operational wavelength of 9.11  $\mu\text{m}$  is a NASA baseline specification and was determined based on signal maximization and eye safety issues.

System Efficiency. The significant measure of performance for the LAWS Optical Subsystem is the heterodyne efficiency budget shown in Figure 6. As indicated, the top level value of .055 represents the ratio of the heterodyne signal power of the LAWS system to the signal power of an ideal system. Included in this value are the terms due to the pupil obscuration and finite aperture clipping, the optical system throughput, polarization mismatch, detector quantum efficiency, and heterodyne detection efficiency. The quantum efficiency used for this calculation of overall efficiency is 55 percent. This represents what would be achievable for a detector with moderate bandwidth in a system that uses some degree of Doppler compensation in the receive local oscillator. The overall heterodyne efficiency for the unstable resonator transmitter illumination, the transceiver aperture with near-center obscuration, transceiver wavefront error of 0.07  $\lambda$  rms, and a pointing error of 1.5  $\mu\text{rad}$  is 0.16.

The requirement for an accessible pupil comes from the need to accurately align the return beam with the local oscillator. The only way to make the return and the local oscillator beam collinear while matching the wavefront tilts of each beam using only one mirror, is to locate that mirror at a pupil image.

Concept. The LAWS Optical Subsystem is divided into two principal assemblies: the telescope (Figure 7) and the relay optics (Figure 8). This choice was made because a system that meets all of the performance requirements using only a three mirror telescope design is not practical. There are not enough degrees of freedom with only three mirrors to produce a system that is diffraction-limited over a 1 deg field of view with the telescope providing the total system magnification. The problem is compounded with the requirements for a well corrected pupil and a flat field. The baseline configuration is split into two parts, allowing a reduction of the magnification of the telescope (which produces a workable telescope design) followed by the relay optics yielding the remaining magnification. This optical configuration represents an optimal compromise between heterodyne efficiency and complexity as determined by the number of optical components.

The baseline optical design of the telescope, shown in Figure 7, is a three mirror eccentric afocal Cassegrain with a 12x magnification that produces a 14 cm diameter beam at the pupil image. The baseline design is an eccentric in-field, three mirror Cassegrain. This means that the intermediate image created over the full 1 deg field of view is displayed slightly above the center line of the telescope aperture, as can be seen in Figure 7. This

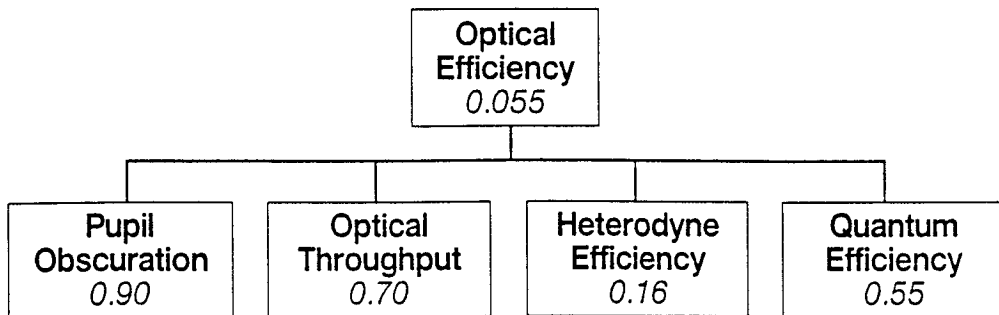


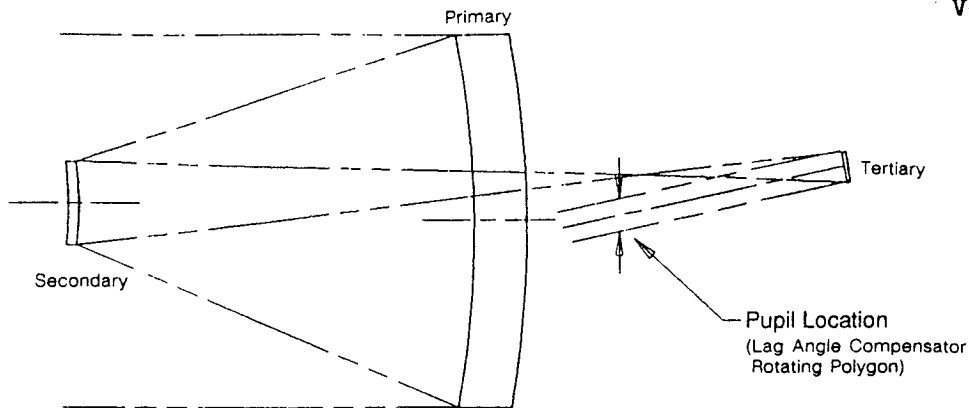
Figure 6. Optical Subsystem Efficiency Budget

has two primary effects. The first is to slightly decenter the secondary; and the second is to form a pupil image slightly below the aperture center line. The first effect has little or no impact on the heterodyne efficiency, and the second provides an accessible pupil where the lag angle compensator can be placed without obscuring the beam. This design is preferable to a concentric design because a concentric design would locate the pupil and the lag angle compensator in the middle of the converging beam, creating a very large obscuration.

The relay optics of Figure 8 form the second part of the total Optical Subsystem, providing the full 42x magnification. This design uses three parabolas to reduce the beam diameter from 14 cm exiting the telescope down to the final 4 cm diameter and then to focus the beam on the heterodyne detector/receiver. Like the telescope, there is an accessible pupil where a tip/tilt mirror is used to remove the residual lag angle which is expected to be on the order of 1 mrad.

The structural design of the LAWS Optical Subsystem is shown in Figures 7 through 9. The telescope assembly of Figure 7 and the gimbal assembly of Figure 9 interface with each other. The telescope assembly is a graphite epoxy shell supporting ULE optical elements, the largest of which is the 1.67 m diameter lightweight ULE primary mirror.

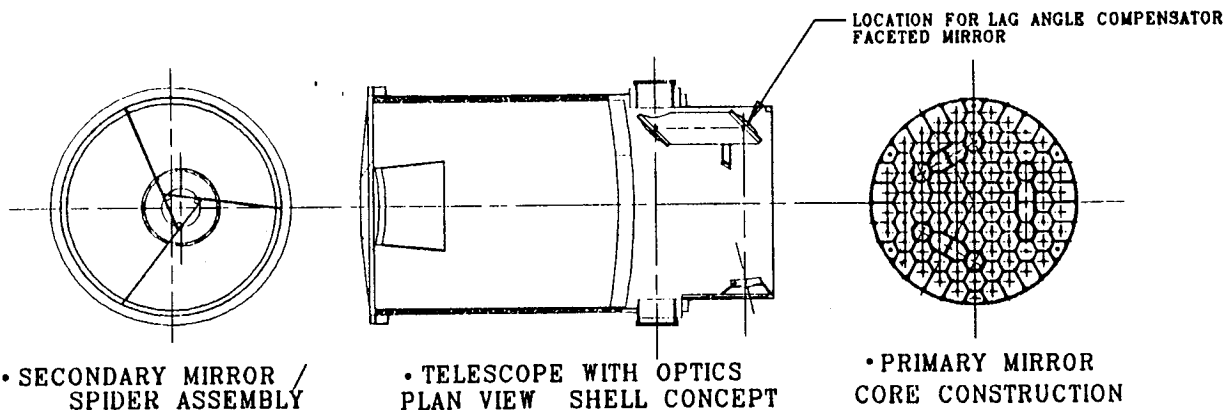
Three materials were evaluated for the optics: ULE, beryllium, and silicon carbide. Because of the mismatch between the thermal coefficients of expansion for graphite epoxy and beryllium, the choice of materials was narrowed to ULE and silicon carbide. ULE was chosen over silicon carbide



Field of View	1° Circular	Surface Specifications:		
Wavelength	9.11 μm			
Magnification	12X			
Obscuration	7%			

LAWS 5-44

(a) Telescope Schematic



• SECONDARY MIRROR / SPIDER ASSEMBLY

• TELESCOPE WITH OPTICS PLAN VIEW SHELL CONCEPT

• PRIMARY MIRROR CORE CONSTRUCTION

#### DESIGN REQUIREMENTS / SPECIFICATIONS

- Allowable WFE ~ 0.07 λrms operational; λ0.014 rms fab/align
- Thermal control power 110 watts; weight 2 kg
- Weight 107 kg; frequency 200 Hz
- Modular design / limited space envelope
- Launch dynamics; 30 g - quasi static load; Telescope locked during launch
- ULE Optics, graphite epoxy metering structure
- Trunnion mounted, center of gravity to within 2 mm of AZ/EL axes

(b) Telescope Assembly

Figure 7. LAWS Telescope Configuration

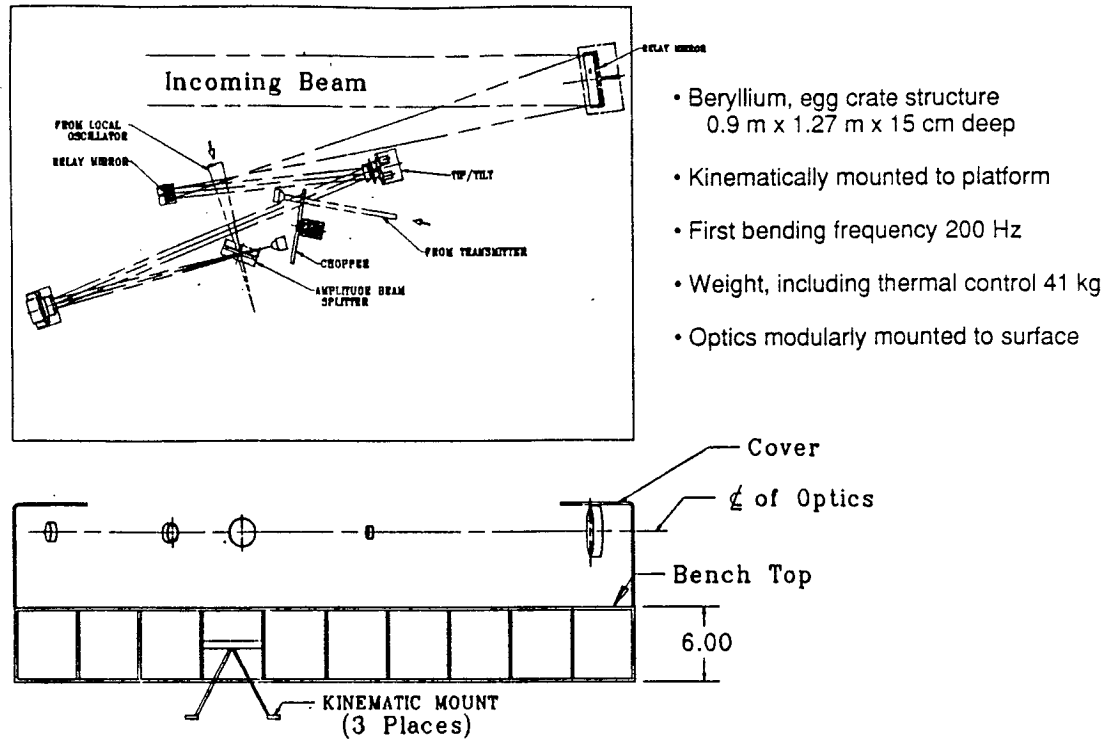
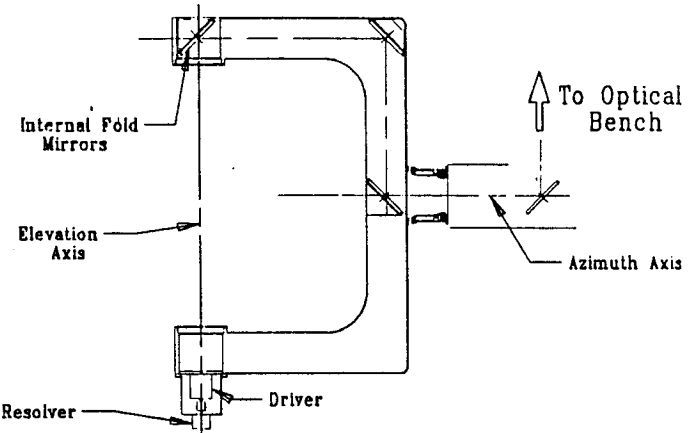


Figure 8. Optical Bench Assembly



#### DESIGN REQUIREMENTS/SPECIFICATIONS

- Elevation angle range 30 - 60 set and hold / elevation drive
- Azimuth Scan - continuous rotation at 6.8 rpm / azimuth drive
- 0.6  $\mu$ rad allowable tip/tilt
- Weight 26 kg; frequency 50 Hz
- Material - Beryllium
- Power consumption - 4 watts

Figure 9. Gimbal Assembly

because of Itek's experience with the manufacturing of large lightweight ULE optics.

The Coudé path which transfers the radiation between the telescope and relay optics is shown in Figures 7 and 9. The mirror to the left of the pupil image (Figure 7) is used to direct the beams through the elevation bearing towards the fold mirror located inside the gimbal portion of the elevation bearing (Figure 9). In Figure 9, two more mirrors direct the beam through the gimbal and then down through the azimuth bearing; the beam is then folded by another mirror out of the gimbal onto the optical bench. As well as housing the Coudé path the gimbal assembly provides the functions of scanning the telescope and varying the elevation angle. This structure is manufactured of beryllium to achieve the highest structural frequency for the lowest weight. The structural requirements for the gimbal are also derived from the line-of-sight error budget.

Attached to the gimbal is the beam scanner (motor/bearing) assembly. This assembly allows the beams to pass through unaffected while rotating the telescope and gimbal assemblies.

The optical bench assembly (Figure 8) not only holds the relay optics, but also the isolation switch and the interferometer assembly. The location of the optical bench relative to the telescope and gimbal is dependent on the (not yet finalized) design of the vehicle with which the LAWS system will interface; however, lack of information with regard to the platform is not a drawback at this time since the laser beams entering and leaving the telescope are both collimated beams going through a Coudé path, resulting in some flexibility as to where the bench can be located. Structurally the bench is a 0.9 m x 1.27 m x 15 cm beryllium egg crate. The choice of beryllium was driven by stiffness-to-weight ratio since all the elements must be held rigidly in place.

The optical bench assembly also holds the interferometer assembly. This assembly performs the function of combining the local oscillator with the return beam. This is performed using a simple amplitude beam splitter that reflects 96 percent of the return beam off the front surface towards the receiver and transmits 4 percent of the local oscillator beam towards the receiver.

In summary, the LAWS Optical Subsystem is a three mirror eccentric afocal telescope which is supported by a graphite epoxy structure, itself supported and rotated by a beryllium gimbal. The radiation that is directed to and from the telescope passes through a Coudé path inside the gimbal towards the beryllium optical bench which supports the isolation switch, relay optics, and the interferometer assemblies. Lag angle compensation is performed by a rotating polygon at the telescope's exit pupil, and the residual lag angle is removed by a tip/tilt mirror located on the bench.

## 2.2 LASER SUBSYSTEM

The transmitter laser is considered the area of greatest risk for the LAWS program. In order to reduce this risk, Lockheed chose the approach of dual sourcing the laser concept/configuration studies. The two sources selected for these studies were Avco, a leading U.S. source of pulsed carbon dioxide laser technology for coherent measurements, and GEC, a leading

European source of pulsed carbon dioxide laser hardware for military operations. Both subcontractors developed concepts to meet the specifications of Figure 10. GEC selected an electron-beam (e-beam) sustained transverse excitation (TE) laser approach while Avco selected a corona pre-ionized self-sustained TE laser approach for their primary configuration design efforts. Subsection 2.2.1 presents a summary of Avco's approach, and 2.2.2 provides GEC's approach.

### 2.2.1 Avco Research Laboratory (ARL) Transmitter Configuration

Based on the given requirements, conceptual trade studies were performed to arrive at an optimum transmitter architecture that would provide a high laser efficiency and a compact device with the lowest possible weight and long operational lifetime.

- $\leq$  175 kg Weight
- $\geq$  20 J/Pulse
- 1 to 3  $\mu$ sec Pulse Length
- $\geq 10^9$  Pulse Lifetime
- Controllable Pulse Rate up to 8 Hz  
( $\leq$  125 ms between pulses)
- $\leq$  200 kHz Chirp
- $\geq$  5% Wall Plug Efficiency
- Size Compatible with H-II/JPOP and Shuttle/SSF
- Operation at 9.11  $\mu$ m

Figure 10. Transmitter Laser Requirements

An injection initiated power oscillator (PO) architecture was selected over the master oscillator/power amplifier (MOPA) and power oscillator/power amplifier (POPA) approaches. This selection was made because (1) Avco has demonstrated the capability to maintain single longitudinal, single transverse mode operation with acceptable frequency chirp using the PO configuration; and (2) the PO is inherently more efficient and compact than either the MOPA or POPA architectures.

Three options were also considered for obtaining single frequency operation of the power oscillator: (1) hybrid gain cell, (2) Fabry-Perot etalon, and (3) injection seeding. The hybrid gain cell was excluded because of size, dual flow loop, and synchronized discharge complexity considerations. The Fabry-Perot etalon was discarded because of difficult alignment problems with multiple passive elements inserted into the cavity and also because of the insertion losses associated with this method as well as the associated added potential for optical path degradation over the life of the laser. The injection seeding approach was selected because of previous success with this optimal approach on the LOKATER program.

Figure 11 shows the basic injection locking scheme. With this technique, the laser resonator is length-tuned until the Fabry-Perot resonance matches that of the injection source. When the transmitter laser is pumped, the selected mode builds from the injection seed rather than random noise. A CW laser, such as a waveguide laser, is used as the injection source. Cavity matching will be performed by locating the resonances of the cold cavity. A PZT drive on a light-weight resonator mirror in conjunction with a closed-loop servo system and the injection laser is used to find the resonance position.

Injection seeding also provides a convenient method of controlling the amplitude of the gain switched spike in the laser pulse. The spike can be reduced by increasing the intensity of the seed signal. This is important for the LAWS transmitter, which requires that the pulse energy be available for Doppler measurement of the wind velocity.

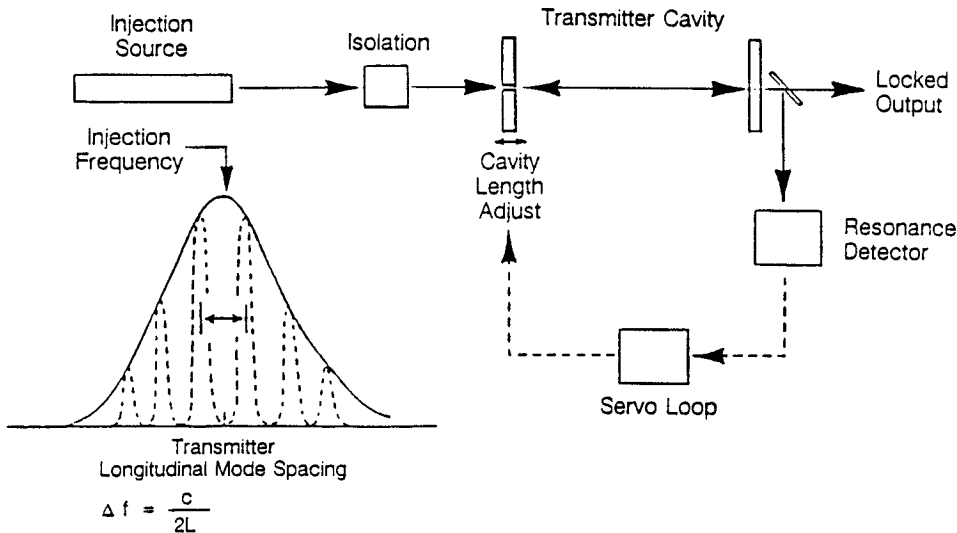


Figure 11. Schematic of the Injection Locking Method

Kinetics codes were used to predict laser performance under selected operating conditions and for our selected CO<sub>2</sub> laser line. The input parameters to the kinetics code are specific energy loading in the gas, mixture composition, pressure, pulse length, and cavity feedback. On the basis of these inputs, the code calculates the specific optical energy output in J/L. The temporal profile of the pulse gives quantitative information about the amplitude and the width of the gain-switched spike, which is then optimized by controlling the intensity of the seed beam.

The specific energy loading has a major impact on the size of the laser because the laser volume scales inversely with this parameter. The size of the flow and acoustic components, flow velocity, and overall weight and volume are driven by the selected discharge loading. A high specific loading is desirable for a low weight and a compact device. A high loading is, however, also detrimental to the stability of the discharge and hence must be tightly controlled. ARL's experience shows that higher specific loadings can be tolerated for short pulse lengths (< 3μsec). ARL has demonstrated streamer-free discharge operation at specific loadings as high as 300 J/L-atm. For the LAWS kinetics trades, conservative values were chosen between 100 and 175 J/L-atm. Conservative loadings provide reliable operation and yet result in a device that will meet the weight specification.

Gas Mixtures. From initial studies, the optimal gas mixtures fall in the range of 50 to 75 percent He and 10 to 25 percent CO<sub>2</sub> with the rest being N<sub>2</sub>. For the required output, an operating pressure near 0.5 atm and a gain length of 150 cm were required, with the discharge loading limited to a maximum of 175 J/L-atm.

Further optimization of the mixture was undertaken to attain the highest efficiency. This study was conducted for three different pulse durations: 2, 3, and 5μsec. For each pulse duration, efficiency was determined as a function of the concentration of N<sub>2</sub>. For pulse durations of interest the efficiency is relatively insensitive to the fraction of N<sub>2</sub> with the N<sub>2</sub>:CO<sub>2</sub> ratio varying from 1 to 2. The maximum efficiency is obtained with a 1 CO<sub>2</sub>:1 N<sub>2</sub>:2 He mixture for the given parameters. Experience with similar devices has shown the 1:1:2 mixture to provide good laser performance. The maximum extraction efficiency (near field) is between 10 and 11 percent.

Optical Resonator. Two fundamental issues were addressed in the performance of trade studies for the optical resonator: (1) the energy delivered into the far field; and (2) the control of transverse mode.

A high magnification is desirable for maximum far-field energy. But higher magnification can only be obtained at a sacrifice of the extraction efficiency. It is these two parameters in conjunction that determine the net far-field energy. Our present design point is at magnification = 2.25, where the far-field energy efficiency is at its maximum.

Mode Control. Obtaining single transverse mode (STM) in the laser output is most important for a coherent pulsed lidar. This is achieved by a judicious choice of the equivalent Fresnel number ( $N_{eq}$ ).  $N_{eq}$  depends on the cavity length (L), the magnification (M), and the radius of the beam. Normally, the aperture is primarily determined by energy considerations with the wave length given. The two variables M and L can be changed to arrive at the desired Fresnel number. Earlier studies concluded that there is a quasi-periodicity in the mode losses as a function of  $N_{eq}$ , such that the mode crossings (where the laser output is known to have mode degeneracy) occur very near to values of  $N_{eq} = n$ , where  $n$  is an integer; the maximum mode separation points occur at values of  $N_{eq} = n + 0.5$  for circular mirrors and at  $N_{eq} = n + 0.4$  for square mirrors. However, there is some weakness in these conclusions since they are based on studies which assumed perfectly aligned mirrors. Recent studies found that mirror alignment had a noticeable effect on the cavity losses for the different modes. If a mirror is tilted even by a small angle such as 10  $\mu$ rad, the mode loss patterns change significantly. Consequently, the effect of mirror misalignment must be addressed carefully during the detailed design phase.

Chirp/Frequency Control. There are a number of processes that can cause the frequency of the output of a pulsed CO<sub>2</sub> laser to vary in time (i.e., cause chirp). In general, offending processes produce time dependent perturbations of the index of refraction of the lasing medium. A new chirp modeling theory has been developed by ARL and experimentally verified. The principal mechanism governing chirp is the heat deposition in the medium due to V-T transfer which results in a change in the index of refraction of the medium. By changing the pressure and composition of the gas mixture, one can significantly alter the lower level relaxation rate and thus control the chirp. Further, it has been experimentally determined that discharge induced chirp in lasers of this general Avco design is negligible.

Initial estimates of LAWS chirp were based on a simplified Rigrod calculation, in which the intensity profile of the laser output is assumed to be Gaussian. This approach normally provides a pessimistic estimate for the chirp, because the extraction-induced heating is higher in the resonator core region where the chirp is generated. More precise wave calculations show that, for the proposed LAWS laser resonator, the maximum intensity occurs at the wings instead of the core region of the gain medium. This results in a lower chirp than initially estimated.

The salient features of the ARL resonator design are identified below:

- Discharge cavity consists of a primary mirror and a light-weight feedback mirror
- Feedback mirror has PZT driven mount for cavity matching
- Gain median is split into two for a compact package
- Intercavity plane blazed grating for line selection
- An injection laser separate from the local oscillator to allow optical isolation between the local oscillator and the power oscillator
- Injection through a 98 to 99 percent reflective turning mirror
- Primary mirror is passive cooled; other mirrors are liquid cooled.

Numerical design parameters are depicted in Figure 12.

<u>Resonator</u>	<u>Flow System Parameters</u>	<u>Pulse Power Requirement</u>
Confocal Unstable	Input Energy/Pulse - 95 J/L	Energy Stored - 262 J
Resonator with Square Mirrors	Energy Out/Pulse - 20 J	Flow Voltage - 20 kV
Equivalent Fresnel Number - 2.4	Cavity Size 4 x 4 x 75 cm <sup>6</sup> (two cavities)	PFN Voltage - 40 kV
Magnification - 2.25	Repetition Rate - 10 Hz	Current - 2.6 kA
Cavity Length - 2.2 m	Gas Pressure - 0.5 Atm	Pulse Duration - 5.0 $\mu$ sec
Gain Length - 1.50 m	Gas Temp - 300 K	PRF - 8 Hz max
Beam Size - 4 cm x 4 cm	Gas Composition - 1CO <sub>2</sub> :1N <sub>2</sub> :2He	Normal Impedance - 7.6 ohms
Radius of Curvature	Cavity Flush Factor - 3	Voltage Rise time - 400 nsec
Primary Mirror - 17.5 m	Discharge Volume - 2.4 liter	dI/dt - $6 \times 10^9$ A/S
Feedback Mirror - 7.7 m		
Loading 175 J/L-atm		

Figure 12. AVCO Laser Baseline Design

Discharge Technique Selection. Avco selected the self-sustained discharge over the e-beam sustained discharge because (1) they have demonstrated low chirp characteristics of a self-sustained discharge of 1 to 3  $\mu$ sec with efficiencies meeting LAWS requirements; and (b) this eliminates what they perceive as the high risk e-beam foil lifetime issues and also reduces required operating voltages. Of the ultra-violet radiation pre-ionizing techniques for gas lasers (i.e., spark board, semi-conductor, UV lamps and corona bar discharges) they have selected the corona bar pre-ionizer as most appropriate for LAWS.

Surface corona is recognized as superior to other types of pre-ionization because of its uniform pre-ionization, its capability for filling relatively large electrode gaps, and its simplicity. A technique has been developed which provides good control over local and volumetric instability phenomena and results in low-chirp discharges at specific energy loadings exceeding 200 J/L per pulses up to 10  $\mu$ sec long. The pre-ionizer is integrated with a perforated plate anode to form a hard flow wall for optimum flow geometry.

Flow Loop. Control of medium homogeneity (i.e., base flow homogeneity) is required for self-sustained discharge operation in that heated gases can provide a high E/N short circuit path for discharge to arc. Thus, thermal clearing of the cavity is required of the flow loop.

Base flow homogeneity is achieved by Avco through proper utilization of flow velocity and temperature control devices such as heat exchangers, passive thermal equalizers, turbulence control screens and honeycomb, and flow control fans. Acoustic quieting between pulses is accomplished by use of mufflers and drag elements. Transient effects caused by initial device turn-on are controlled by active heat exchanger throttling.

The required gas velocity in the cavity is set by the pulse repetition rate and the required flush factor (i.e., how many cavity dimensions downstream the ionized gas must be moved in the interpulse period to avoid interference with the next discharge). Typical flush factors range from 4 to 1 for UV pre-ionized self-sustained discharges. The Avco design LAWS flush factor is 3. Total flow loop volume will typically be between 100 to 200 cavity volumes, dependent upon pulse repetition rate and flush factor.

Several recent design studies at ARL have been focused on compacting laser transmitter designs. The proposed method of compacting the flow system achieves this by utilizing a dual folded cavity concept. With this concept, wasted space in the flow return is virtually eliminated. Compaction is further accomplished by combining element functions and eliminating transition zones between elements. The tangential or cross-flow fan combines a fan, a turn, and a contraction section into one unit. Another compacting concept which has been utilized is a diffusing turn, which combines the functions of the usual vanned diffuser and the vanned turn. The residual thermal energy in the laser gas associated with the pulsed laser operation is removed by the two highly-efficient heat exchangers, while gas thermal fluctuations/variations are controlled by two thermal equalizers. The side-wall mufflers are designed to damp the laser-initiated acoustic disturbances during the interpulse time. Boundary-layer suction is utilized upstream of the discharge region to control the cavity boundary-layer growth. This is achieved by internally venting the discharge region to the suction side of the nearest upstream fan. An on-line catalytic converter is incorporated in the flow loop to regenerate the CO<sub>2</sub>.

The pulsing of the laser discharge causes hot slugs of gas to be formed which must be removed before passage to the following cavity. The skewed heat exchanger inlet causes them to enter the heat exchanger over a substantial portion of that spacing; this greatly smears that non-uniformity. The heat exchanger is, however, conservatively designed to produce temporal ΔT thermal equilibration by four orders of magnitude. At 27 fins per inch, the heat exchanger is 3 cm thick in the flow direction, with a frontal area 3 times the cavity flow area.

The Avco fan choice is a 2 in. tangential fan. The projected operating speed for a total pressure rise of 5 cavity velocity heads and a cavity flush factor of 3 is 710 rpm. The fan will be mounted with shafts leaving the laser gas region through FERROFLUIDIC<sup>R</sup> seals with external bearings and motors sealed in separate enclosures.

The contracting tangential fan is followed by a final ceramic thermal equalizer which provides an additional factor of 2.5 in thermal equilibration, reduces any turbulence scale size, removes any swirl from the fan, and provides a pressure drop of 2 cavity velocity heads, thus further smoothing velocity nonuniformity. This unit is a 4 cm length of ceramic honeycomb with 1 mm square cells. The ceramic can also serve as the support structure for the catalyst.

An effective catalyst that will satisfy the LAWS mission requirements has to meet several criteria: (1) high activity at the ambient gas temperature, (2) minimal degradation of catalytic activity over 3 or more years of laser operation, (3) minimal isotopic oxygen exchange between the catalyst substrate and the lasing medium, and (4) absence of dust or other deleterious by-products of catalyst operation. The most important of these criteria are (1) the catalyst efficiency and its degradation with operating time, and (2) isotope exchange between  $\text{C}^{18}\text{O}_2$  gas and the  $\text{O}_2$  in the catalyst support. The  $\text{C}^{18}\text{O}_2$  catalyst is being developed by NASA but must be tested in the LAWS laser.

Pulse Power. A pulse power system will be required to supply the necessary pumping of the laser gas in the self-sustained discharge mode. The corresponding pulse power system requirements are listed in Figure 12.

The 28 Vdc platform power will be conditioned and stepped up to the required pulse forming network (PFN) charge voltage of 40 kV through a dc/dc converter, consisting of a series resonant inverter, a step-up transformer, and an output rectifier. The PFN will be charged from this power supply unit at a constant current upon command. The PFN consists of passive elements such as capacitors and inductors and stores the energy for the discharge. A full voltage Guillemin PFN is selected for the LAWS Baseline. A thyratron has been selected for high voltage switching..

Figure 13 depicts baseline design power/efficiency parameters for the Avco configuration. Figure 14 depicts an artist's concept of the laser head.

## 2.2.2 GEC Avionics Transmitter Configuration

Discharge. GEC investigated self-sustained, pulser-sustainer (x-ray pre-ionized) and e-beam-sustained discharge lasers and chose the e-beam sustained discharge as their primary LAWS configuration. They stated the primary advantages of this discharge technology as follows:

- Maximum wall plug efficiency
- Reduced catalyst requirement because of lowest  $\text{CO}_2$  dissociation rates
- Less isotopic scrambling because of low dissociation rates
- Near top hat pulse temporal shape with ready control of gain switched spike and no tail (prevents ambiguity from data near clouds)
- Good frequency control from discharge current control during optical pulse
- Arcing due to electron attachment is not an issue (no arcing)
- Demonstrated LAWS output energies (20J/pulse) and sealed-off operation.

<u>COMPONENT</u>	<u>NUMBER</u>	<u>UNIT</u>	<u>TOTAL</u>
<b>1. LASER</b>			
Required Output	20	Joule	
Intrinsic Efficiency	11.5%	-	
Edge Effects	81%	-	
Non-Uniform Pump	90%	-	
Overall Efficiency	8.38%		
Rep. Rate	8	Hz	
Input to Laser	1908	Watt	
<b>2. PULSE POWER SYSTEMS</b>			
Required Output	1908	Watt	
Pulse Modulator Efficiency	81%	-	
DC Power Supply	90%	-	
Overall Pulse Power	72.9%	-	
Prime Power Input	2618	Watt	2618
<b>3. FLOW LOOP</b>			
Required Flow Power	4	Watt	
Fan Efficiency	12%	-	
Bearing Losses	2	Watt	
Shaft Power	35	Watt	
Motor Efficiency	80%	-	
Total Flow Power	44	Watt	44
<b>4. INJECTION LASER</b>			
	50	Watt	50
<b>5. INSTRUMENTATION &amp; CONTROL</b>			
	100	Watt	<u>100</u>
Total Transmitter Power Requirements			2812 Watts
Total Transmitter System Efficiency			5.68%

Figure 13. Baseline Avco Design Power/Efficiency for 20 J/pulse,  
8 Hz Transmitter

They perceive the risks with this configuration to be in the areas of (a) foil lifetime, (b) radiation emission control, and (c) high voltage (106 kV) control.

GEC has developed and operated a test bed with an e-beam sustained amplifier with discharge dimensions similar to LAWS (if configured as an oscillator, an output of 20 J/pulse is expected). The system has been

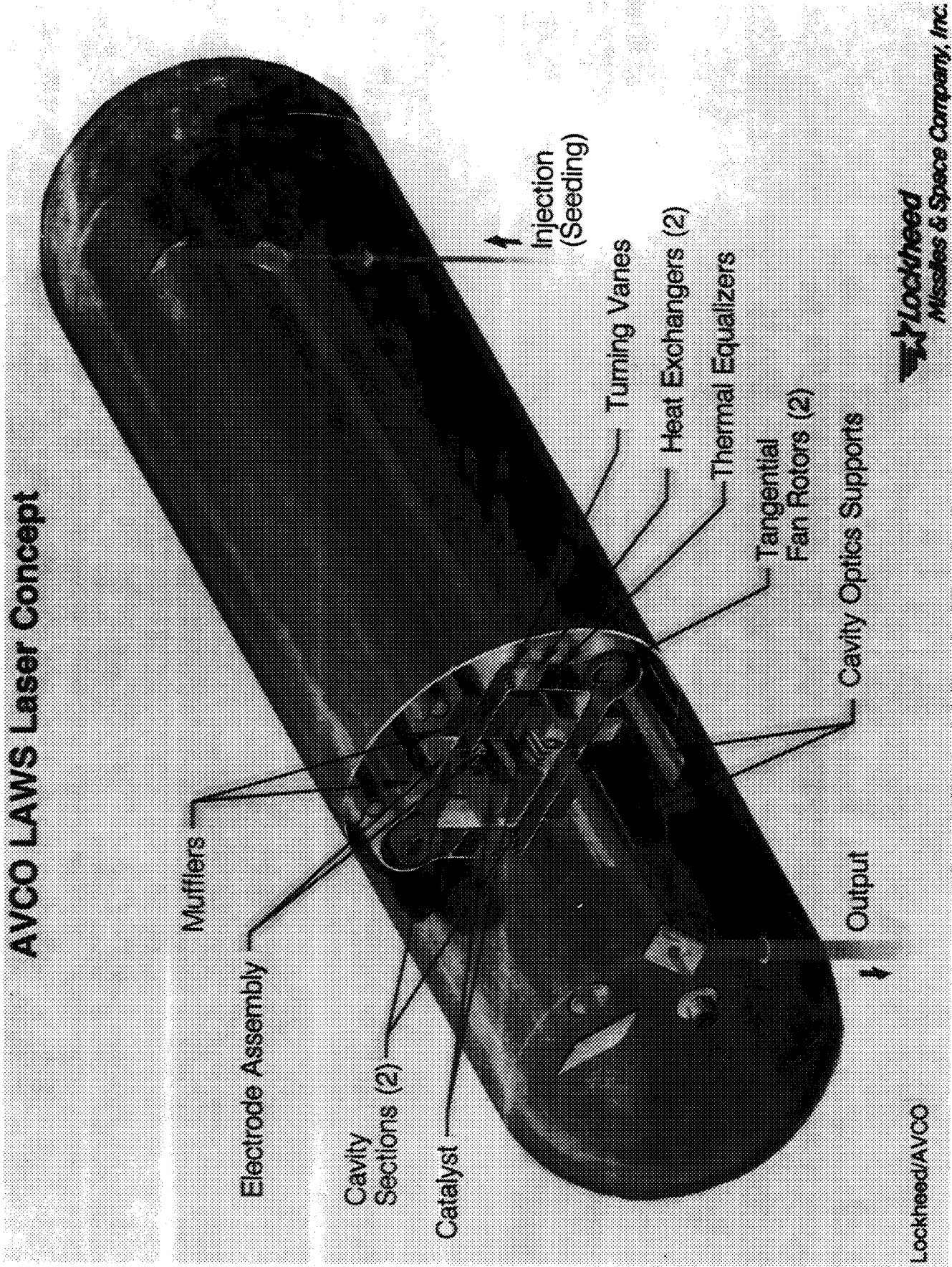
**AVCO LAWS Laser Concept**

Figure 14. Avco Laser Head Concept

operated sealed for over 2 million pulses at 8 Hz with oxygen levels maintained below 0.001 percent and no measurable change in operating parameters. The test was discontinued at 2 million pulses because this exceeded the requirement of the specific funded test. The significance of this test to LAWS was in the demonstrated gas control for a LAWS size discharge.

Frequency Stability. Having achieved oscillation on the correct line and single longitudinal and transverse mode operation, it is necessary for that oscillating cavity mode to remain constant to the required level (to within 200 kHz) throughout the pulse. The cavity resonance condition is  $m\lambda = 2nL$  where  $m$  is an integer, and  $\lambda$  is the wave length. There is thus a requirement on the stability of both the cavity refractive index ( $n$ ) and length ( $L$ ) for the duration of the optical pulse. The refractive index can be altered during a pulse due to contributions from the laser induced medium perturbation (LIMP) and change in the plasma electron density.

In a gas discharge laser, if the discharge current varies, the electron density and thus refractive index of the gain medium will vary. This, in turn, will cause the cavity resonance condition to drift to a different oscillating frequency. For the LAWS laser, the discharge current ripple must be held within 50 A ( $\pm 1.3$  percent) for the duration of the optical pulse to maintain frequency stability within 200 kHz according to GEC calculations excluded in this Executive Summary.

Likewise, for a LAWS cavity frequency of  $3.28 \times 10^{13}$  Hz (9.11  $\mu\text{m}$ ) and a length of 0.6 m (typical of expected LAWS laser design) then the 200 kHz stability requirement implies that cavity length variation must be controlled to less than a 3.7 nm drift for a 3  $\mu\text{s}$  optical pulse length. Variations to the cavity length can be caused by thermal drift, shock waves, or mechanical vibration of the cavity mirrors. The proposed GEC optical resonator will be mounted on three multiply carbon fibre tubes with a temperature coefficient in the longitudinal direction of less than  $0.02 \times 10^{-6}\text{K}^{-1}$ ; the temperature of the laser structure will be held constant to better than 0.3  $^{\circ}\text{C}$  for the duration of the 3  $\mu\text{sec}$  optical pulse.

The pressure shockwave from the discharge will travel at less than 1 mm per  $\mu\text{sec}$  and will not affect the mirror position during the optical pulse. However, the mirror mounts will be designed to damp out any oscillation caused by this shockwave in the interpulse period. Similarly, the GEC cavity mount is designed to be decoupled from external vibrations and to be stiff enough to resist oscillating driving forces. Analysis has shown that it is unlikely that acoustic vibrations from the fan will adversely affect the laser frequency stability.

The LIMP in a CO<sub>2</sub> laser occurs due to the faster relaxation of the lower laser level over the upper laser level, leading to a gas heating rate related to the intracavity intensity. This gas heating causes an adiabatic expansion and consequent density reduction, thus altering the refractive index of the gas. As the intracavity refractive index changes, so does the resonant frequency of the cavity throughout the laser pulse, leading to an increasing laser frequency or chirp. Theoretical estimations of LIMP-based chirp for LAWS tied to experimental data are presented in Volume II.

Wavelength Selection. Wavelength selection can be achieved either by an intracavity dispersive element or by cavity optics coated to have a high reflectivity only for the required wavelength. The dispersive element approach is chosen because it is a proven technique.

The cavity optics coating is rejected because (1) coating with such narrow band reflectivities will be difficult if not impossible to fabricate; if it could be fabricated, the coating would consist of many layers; and (3) the coating would exhibit less than optimal reflectivity for LAWS leading to reduced efficiency.

Single Longitudinal Mode. The essence of SLM operation is to have only one cavity mode frequency within the laser medium bandwidth with a round trip gain greater than the cavity losses. This situation can be achieved by using a cavity with wide mode spacing (implying short cavity length) and a laser medium with a narrow gain bandwidth (obtained by operating the laser at a reduced pressure). Other techniques can be applied to select only certain cavity modes by reducing the cavity losses on these modes only. These methods include the use of intracavity etalons, low pressure discharges, and three-mirror cavities. A modified three mirror approach is selected for LAWS with the inner mirror being a lens, and one end mirror being a grating, as is discussed below under Resonator Configurations.

Single Transverse Mode. For a stable cavity, the normal method of producing STM oscillation is to use an intracavity restricted aperture. This increases the losses of higher order modes, while keeping the losses low for the TEM<sub>00</sub> mode. This mode has a Gaussian profile and thus the majority of its energy concentrated along the cavity axis. For the LAWS laser it will not be possible to use a small intracavity aperture as this conflicts with other system requirements such as the need for low frequency chirp due to LIMP.

The unstable resonator configuration selected by GEC for LAWS has an inherent selectivity for oscillation on a STM for a correct choice of cavity parameters. Since an unstable resonator also allows efficient extraction of energy from a large gain volume, it also provides a good method for STM oscillation.

Resonator Configuration. The two major options available for the design of the LAWS laser are either to imbed the wavelength and mode selection elements in a PO, or to decouple the frequency selection and energy production parts of the laser into a separate master oscillator and power oscillator, respectively. The master oscillator is then used to injection seed the power oscillator. (A sequential MOPA configuration option is rejected due to a well known low overall efficiency because of a resultant poor energy extraction from the amplifier stage.)

The standard PO configuration replaces one cavity mirror with a curved grating used in the Littrow orientation. However, this leads to astigmatism in the cavity mode and output beam. Astigmatism is overcome in GEC's approach by producing plane wavefronts to enable a plane Littrow mount grating to be used. This is achieved by placing a lens in front of the grating. If the surfaces of the lens are made partially reflecting, then several advantages of

this system are realized. First, the energy density on the grating is reduced, protecting it from damage. This technique has been used in line tuned CO<sub>2</sub> lasers employing plane-plane cavities to produce high energy pulses over a wide range of lines. Second, a short length resonator is formed between the grating and the lens. This has a wide resonator mode spacing. The total laser cavity would only oscillate at those frequencies where the cavity resonance condition was fulfilled for both resonators simultaneously with both within the active medium gain bandwidth. Thus, this three-element cavity produces both line and longitudinal mode selection. In this configuration, the short resonator length is controlled to keep its frequency matched to the long resonator mode closest to the laser line center. At the same time the long resonator length is controlled to keep the resonator frequency within a predetermined maximum offset from the system local oscillator frequency.

A hard-edged uniform reflectivity mirror (URM) unstable resonator provides better energy extraction from the laser gain medium than one employing Gaussian reflectivity mirrors (GRMs), as shown in Volume II. GEC recommends the URM.

Injection Seeding. In the injection seeded configuration proposed by GEC, the longitudinal mode and line selection functions of the system are performed in a MO which is then used to seed the PO to produce high energy oscillation on the required line, with single longitudinal mode. Although the PO has the same wavelength as the MO, it will not have exactly the same frequency. The proposed MO will not have enough power to lock the PO modes to its frequency, but will preferentially seed the PO mode closest to its frequency; this mode will dominate the PO output. The MO must not be allowed to oscillate midway between two PO modes as this could cause dual PO mode output. Also, the chirp requirement on the MO is relaxed in that as long as its frequency does not vary by more than one half the PO mode spacing, single longitudinal mode output from the PO should be possible. For a 60 cm PO resonator length, there is only a requirement to hold the MO chirp to less than 100 MHz.

Two options are available for injection seeding: continuous wave or pulsed MO. A continuous wave MO will be more easily frequency stabilized with respect to the system LO, but a pulsed MO will be able to provide a greater energy density of seed radiation in the PO.

The injection seeding process can be assisted, reducing the MO power required, by increasing the intracavity loss for undesirable wavelengths. This can be achieved by coating the cavity optics for high reflectivity for R branch transitions of Cl<sub>18</sub>O<sub>2</sub> and low reflectivity for P branch.

Work undertaken at Heriot-Watt University on injection seeding a long pulse 3 J laser with a stable cavity has shown that it is possible to produce single line output for a number of lines in both the 9 μm and 10 μm bands of the Cl<sub>18</sub>O<sub>2</sub> isotope using 10 to 20 mJ of injected energy. For a 20 J PO laser, it is estimated that it will be necessary to produce 100 mJ of line-tuned, single longitudinal mode energy from the MO. GEC Avionics has

extensive previous experience in producing line tuned TEA laser oscillators at the 100 mJ energy level. From that work, and a large knowledge base in mini-TEA lasers, a design outline of the MO can be made. Using an injection seeded arrangement increases the LAWS laser efficiency from 7.3 percent for a dispersive cavity to 8.8 percent using an e-beam sustained discharge.

Two options for injection seeding are considered: (1) hole in the cavity mirror, and (2) off-axis injection. For the hole method, the MO beam is directed through a hole of a few millimeters diameter in the rear cavity mirror of the PO. This method had been successfully used at GEC Avionics, though not for a frequency stable laser. There is some evidence that the cavity transverse mode structure can be distorted in this scheme. An additional problem is PO laser radiation escaping through the hole and causing frequency pulling of the MO, requiring an optical isolator.

Injection seeding using radiation not injected exactly along the laser cavity axis has been demonstrated at Heriot-Watt University. As long as the off-axis injected radiation makes a single pass through the gain medium, it can injection seed the laser cavity. This scheme, with the MO not aligned with the PO cavity removes the need for an isolation device between the two oscillators, as no high energy laser radiation is coupled into the MO. This method therefore forms the GEC baseline scheme for the injection of the MO radiation into the PO cavity.

Foil Lifetime. Careful consideration must be given to the design of the foil and the foil support structure of the electron gun if an e-beam sustained discharge technology is chosen for the LAWS laser. A primary concern in these design considerations must be the necessity of obtaining a  $10^9$  pulse foil lifetime. This is an increase of 100 to 1000 times over currently reported foil lifetimes; however, it should be noted that long foil lifetimes were not a major design consideration of prior systems.

The properties required by the foil material are

- High thermal conductivity
- Low electron absorption coefficient
- High ultimate tensile strength
- High endurance limit.

The main materials having these properties are aluminum and titanium, aluminum having a greater thermal conductivity and titanium being stronger. It is possible to combine the properties of the two materials by forming a composite Al:Ti foil. Indeed the longest foil lifetime report to date ( $10^7$  pulses) used such a composite.

Dr. D.V. Willets at RSRE Malvern has performed calculations investigating the thermal loading and mechanical stress effects on the foil lifetime. GEC proposes performing foil lifetime risk reduction activities along the lines outlined by Willets. These are detailed in Volume II.

Radiation Issues. The current design for the LAWS laser proposed by GEC Avionics is an e-beam sustained laser. During the operation of such a laser a 160 kV e-beam is generated, which then passes through a thin metal foil into the laser discharge region. Some of the electrons interact with the foil atoms and X-rays are thus produced at known yields. GEC has ascertained that the resulting X-ray doses will not adversely affect the space platform and its component parts if these have been properly designed to operate in the space environment; only a minimal amount of shielding (designed into the laser itself) is required to reduce the x-ray dose to levels below the natural dosage in the polar orbit.

Electron Gun. The electron gun design is based on a device recently built and tested by M. Harris, RSRE Malvern. The electron gun proposed for LAWS is a simple, ultra-high vacuum design in which the complete envelope is metal held at zero volts. The gas is enveloped by a composite structure comprising carbon fibre material and an internal metal coating for EMI and X-ray shielding. The cathode is an aluminum alloy and is supported on a ceramic high voltage feedthrough. The nickel auxiliary electrode in the field-free drift tube is carried on ceramic-metal hard sealed feedthroughs with knife edge/copper gasket seals.

E-Beam Generation. A continuous low current (5 to 50 mA) dc discharge at a few hundred volts is maintained in the drift section by virtue of the auxiliary electrode. When a high voltage pulse (160 kV) is applied to the cathode, positive ions extracted from the auxiliary discharge are accelerated down the gun to bombard the cathode. Bombardment of the cathode liberates electrons which are accelerated up the gun to form the e-beam.

Pulse Forming Network. The GEC laser pulse forming network produces a square pulse of nominally 6  $\mu$ s pulse width. This is achieved using a five mesh network, each mesh consisting of an equal value of inductance and capacitance. At the two ends a slightly larger inductance may be used to avoid mismatch and smooth out ripples. The total inductance is 48.4  $\mu$ H and the capacitance 0.19  $\mu$ F. The discharge current is 1532 A and the charging voltage 49 kV. These figures were used to determine the weight and size of the capacitors and inductors. The laser PFN is discharged by the laser itself, responding to electrons from the electron gun.

The electron gun pulse forming network produces a nominally square pulse of 8  $\mu$ sec pulse width. This is also achieved using a five mesh network. The total inductance for the gun PFN is 877  $\mu$ H and the capacitance 18 nF. The discharge current is 7.3 A and the charging voltage 32 kV. The gun PFN is discharged by the thyratron switch which discharges into the pulse transformer. The pulse transformer is required to step up the voltage from 16 kV to the necessary 160 kV for the electron gun.

Assuming a total capacitance of 0.19  $\mu\text{F}$  has to be charged to 49 kV at a repetition rate of 8 Hz, a power supply of approximately 1.8 kW is required. The power supply is assumed to be 85 percent efficient, which will be achieved using a resonant switch mode supply with a switching frequency of approximately 100 kHz.

Physical Design. The weight, volumes, and power requirements of all individual modules have been estimated, in most cases by analyzing the design to component level. The modules have then been arranged to form a compact Laser Subsystem. These design guidelines are summarized in Table 1.

A block diagram of the Laser Subsystem is shown in Figure 15, the modular arrangement is shown in Figure 16, and an outside view is shown in Figure 17. A concept of the laser head cross section is depicted in Figure 18.

System power and weight summaries are shown in Figure 19.

### 2.3 RECEIVER/PROCESSOR SUBSYSTEM SUMMARY

The Receiver/Processor Subsystem has the following characteristics:

- Quad HgCdTe photovoltaic detector array with 50 percent quantum efficiency at 300 MHz bandwidth (BW)
- Signal aligned on central element of array with exterior elements for alignment monitoring
- Two-stage phased electro optical modulator local oscillator to reduce detected BW from 1.35 GHz to 0.3 GHz
- Local oscillator beam tailored for shot noise limited operation with phase front matched to signal beam
- Split Stirling Cycle cryogenic cooler to optimize detector operating temperature
- Bias supply and preamplifiers space qualified versions of standard units
- 12 bit 50 MHz analog-to-digital converter for adequate frequency response and dynamic range
- Optional on-board FFT processor for real time velocity data.

Table 1. GEC LASER SUBSYSTEM DESIGN GUIDELINES

- All high voltage connections are bulkhead to bulkhead plug/sockets to minimize EMI emissions. This eliminates high voltage wires between modules.
- Each module is an individually screened metal enclosure. No current passes through the outside of enclosures.
- Both laser electrodes are isolated from the laser enclosure.
- Modules to be kept close together to minimize laser current loop and hence radiated magnetic fields.
- The electron gun is positioned immediately above the laser to permit entry of electrons.
- Some currents will flow around the foil and drift tube area.
- The electron gun vacuum chamber should be covered with an insulator, outside of which there should be another metal enclosure to provide EMI screening.
- The screening is also adequate to reduce emitted X-ray radiation to below the background level for orbits passing polar regions.
- Transformer size can be obtained by combining the core and coil which overlap.
- Position transformer immediately next to gun to prevent any wires carrying 160 kV.
- Master oscillator laser head should be near the large laser to minimize length of laser beam connection.
- Master oscillator pulse forming network should be near to the laser head for minimum inductance and EMI screening.
- Pulse forming network should be at the opposite end from the laser output to allow space for high voltage leadthroughs.
- The master oscillator and electron gun should both operate at 32 kV so they can use the same high voltage power supply. They may also be able to use the same switch. This is a high risk option at present as the delay between the two lasers would be fixed. Two switches have therefore been included.

Table 1. GEC LASER SUBSYSTEM DESIGN GUIDELINES (Concluded)

- The master oscillator switch should be adjacent to pulse forming network for EMI containment.
- The electron gun PFN is adjacent to transformer to minimize lead lengths.
- The electron gun switch is next to the gun PFN.
- The electron gun high voltage power supply unit is adjacent to gun switch or gun PFN.
- The electron gun high voltage power supply unit is adjacent to master oscillator switch of PFN.
- The thyratron power supply is adjacent to both switches to prevent power losses in high current lines, and to minimize weight of thick wires.
- The auxiliary discharge power supply is adjacent to the electron gun.
- Spare space at output end of laser transmitter is used for control/ diagnostics and connects to LAWS Instrument.
- These should be EMI shielding/housing around modules.
- There will be a high tolerance on the output beam stability with respect to the laser mounting face.
- Therefore, the number of components between the mounting face and the optical resonator should be minimized.
- The laser head is mounted directly on Laser Subsystem mounting face.

The LAWS Receiver/Processor Subsystem consists of a modest BW photo detector array, an active cooling apparatus for the photo detector, bias circuitry, preamplifiers and on-board signal processing electronics. For each of these components, several options were considered. These options are outlined in Volume II, Section 5.2.3, along with the logic for selection of the baseline Receiver/Processor Subsystem components.

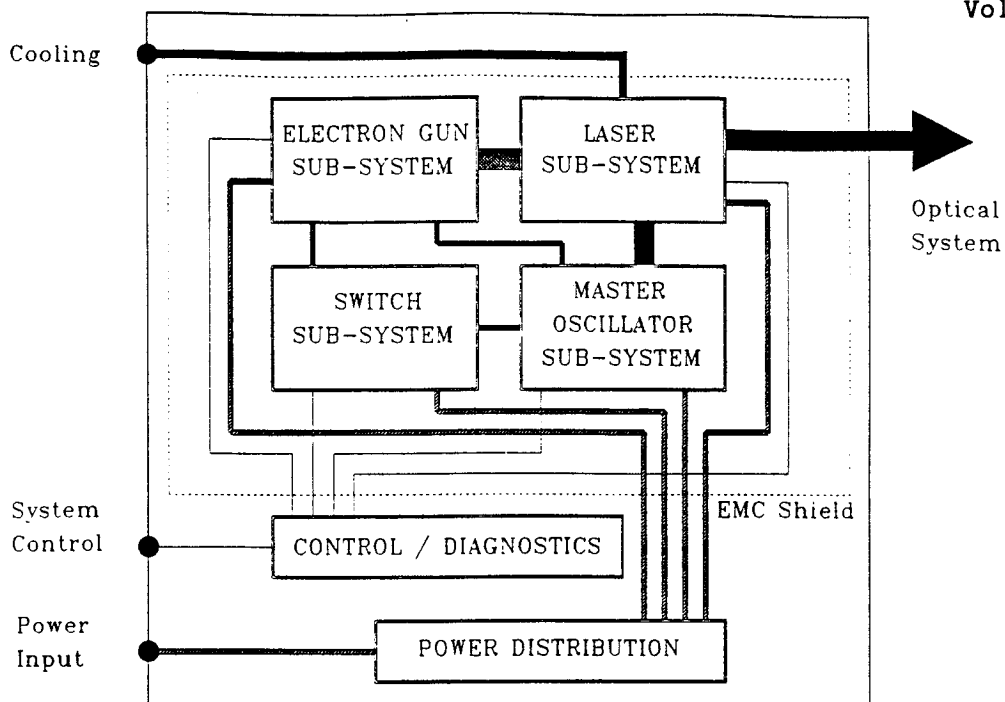


Figure 15. GEC's LAWS Laser Subsystem Block Diagram

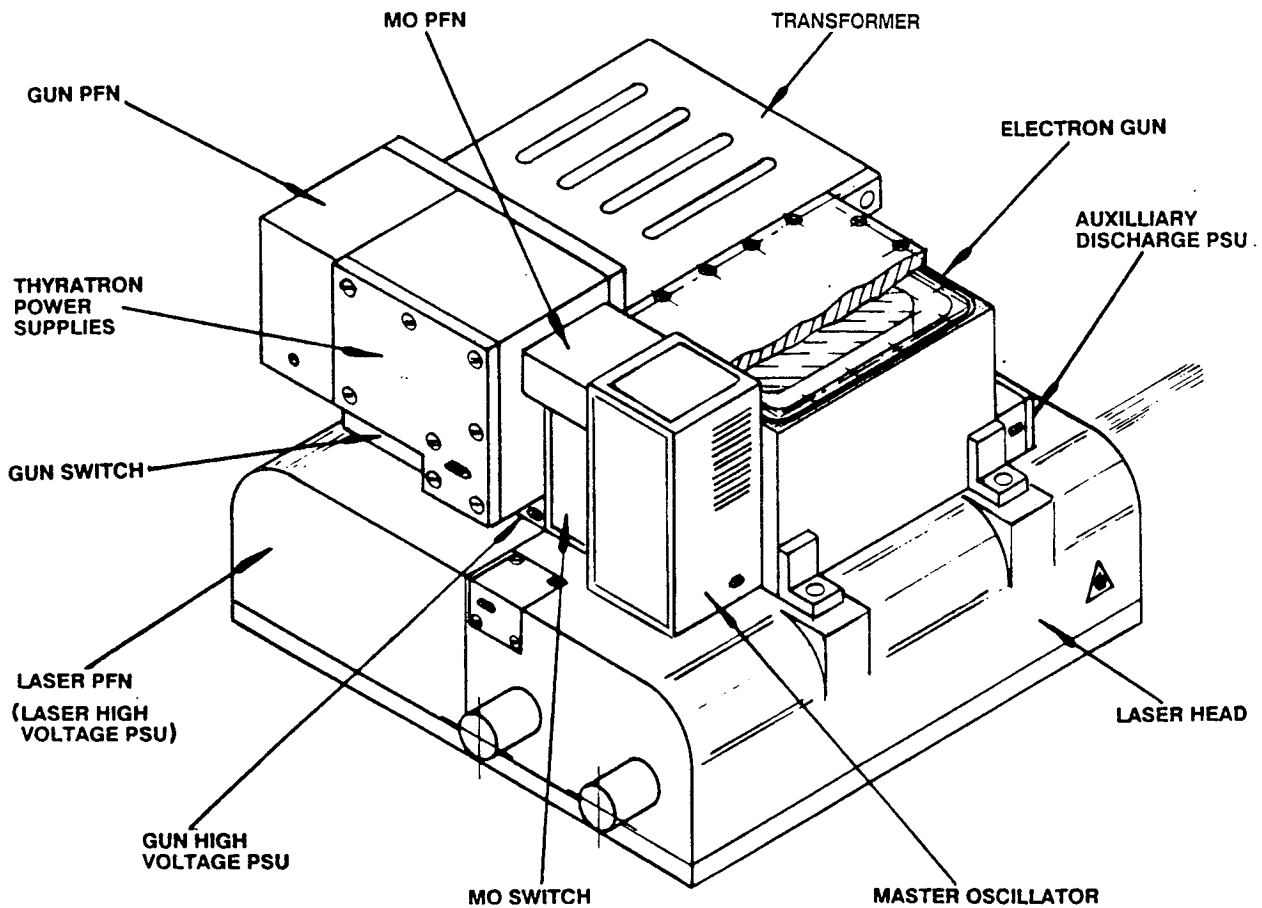


Figure 16. GEC's LAWS Laser Subsystem Modular Arrangement

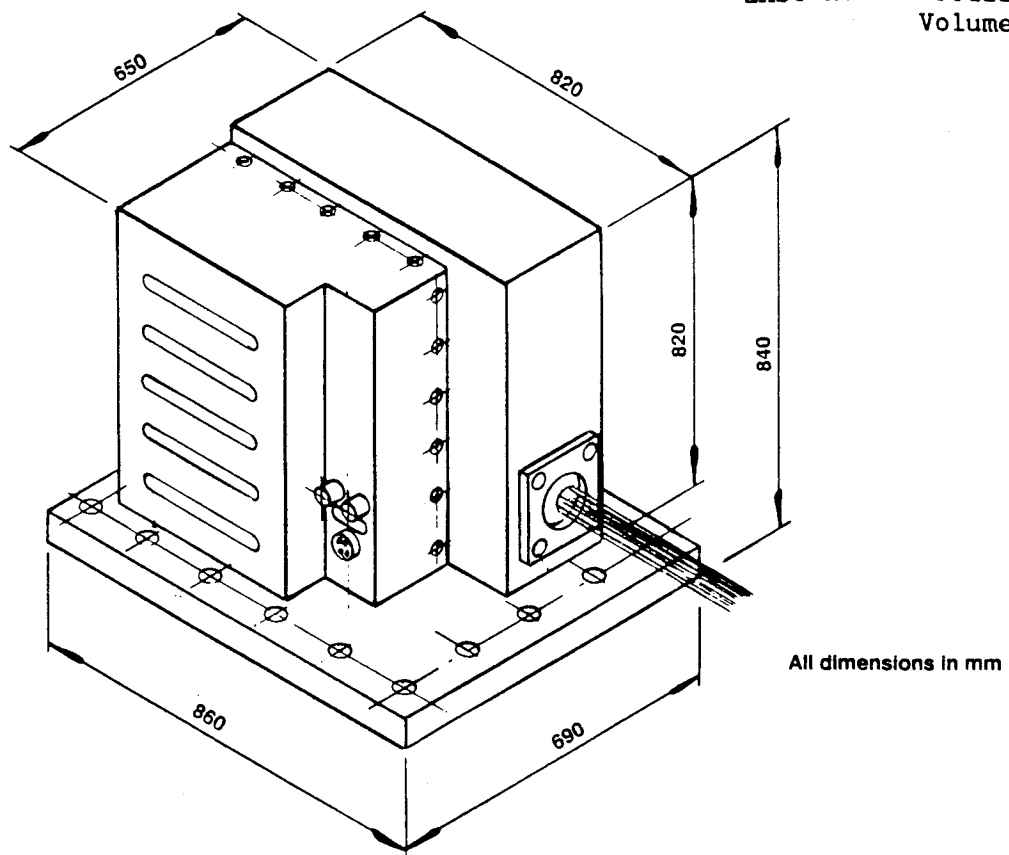


Figure 17. GEC's LAWS Laser Subsystem External View

Figure 20 depicts the Receiver/Processor Subsystem in block diagram format. The local oscillator optical source (upper left hand corner of figure) from the master oscillator is fed into the modulator, where it is up/down shifted before being focused upon the photo detector. The Doppler signal is received from the telescope and optical train and also directed toward and focused upon the photo detector array. Cooling is provided to thermally bias the detector to an optimal operating point. Outputs from the detector are amplified and frequency biased into an acceptable frequency/amplitude range for the analog-to-digital (A/D) converter. The levels of each channel from the detector array are measured to monitor the received optical signal spot location upon the detector array for optimal alignment. The output of the A/D is buffered and telemetered to the platform data interface or (optionally) directly to earth. On-board FFT processing can also be provided to obtain real-time velocity spectra.

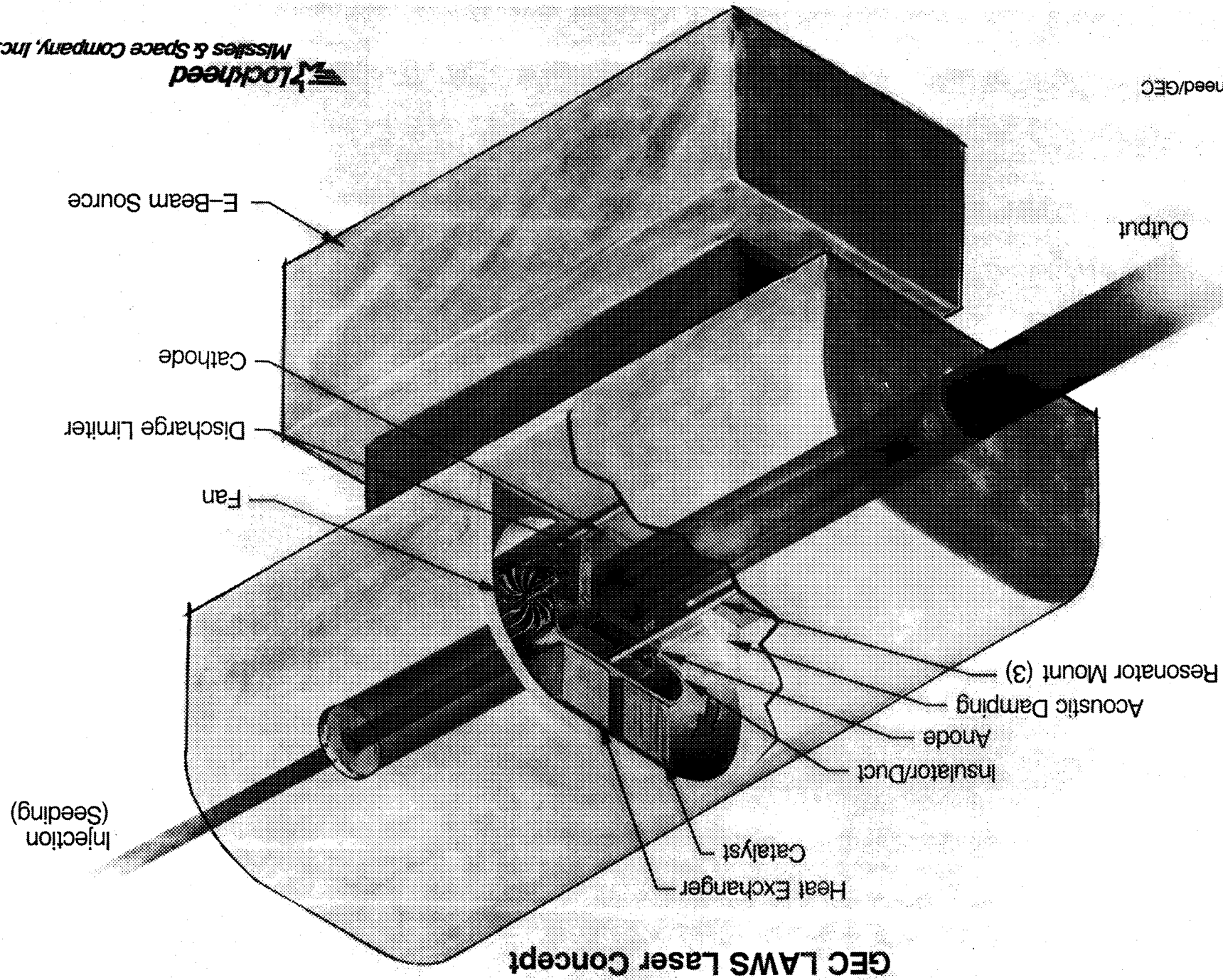
#### 2.4 COMMAND, COMMUNICATION, AND CONTROL SUBSYSTEM

The Command, Communication, and Control Subsystem design is summarized as follows:

- o Hardware implementation
  - Flight computer
  - Communication links
  - Transceiver

FIGURE 18. GEC Laser Head Concept

Lockheed/GEC



Laser power	2139	Laser head	25.9
Electron gun	88	Electron gun	5.3
Auxiliary discharge	15	Laser PFN	45.1
Thyatron heater	378	Laser HVPSU	14.2
Fan motor	40	Electron gun PFN	3.0
Master oscillator	47	Electron gun HVPSU	0.6
Diagnostics and control	10	Switches	6.0
Total power	2717	Thyatron heater PSU	7.7
Wall-plug efficiency (%)	5.9	HV transformer	26.5
		Master Oscillator and PFN	8.8
		Miscellaneous	15.1
		Sub-total	153.5
		Contingency (%)	10
		Total weight	168.9

Figure 19. GEC's LAWS System Power and Weight Summary

- Software modules
  - System management
  - Shot management
  - Communication management.

At this stage of the LAWS Instrument definition process, the emphasis for defining the command, communication, and control of the system is placed on requirements analysis and on definition of associated functions to be implemented and their interrelationships. The Command, Communication, and Control Subsystem encompasses all functions associated with system control, data processing, and communication control. Figure 21 depicts the flight data management and control functional hierarchy. In operation, the function of the Command, Communication, and Control Subsystem is to provide the control of the LAWS Instrument operation and to control communication between LAWS subsystems and between the LAWS Instrument and the host platform. The software required to implement these functions will be incorporated in the flight computer and are identified in Figure 22. Typical data/command interfaces between the LAWS subsystems, environment, and platform are depicted in Figure 23. See Volume II for additional detail.

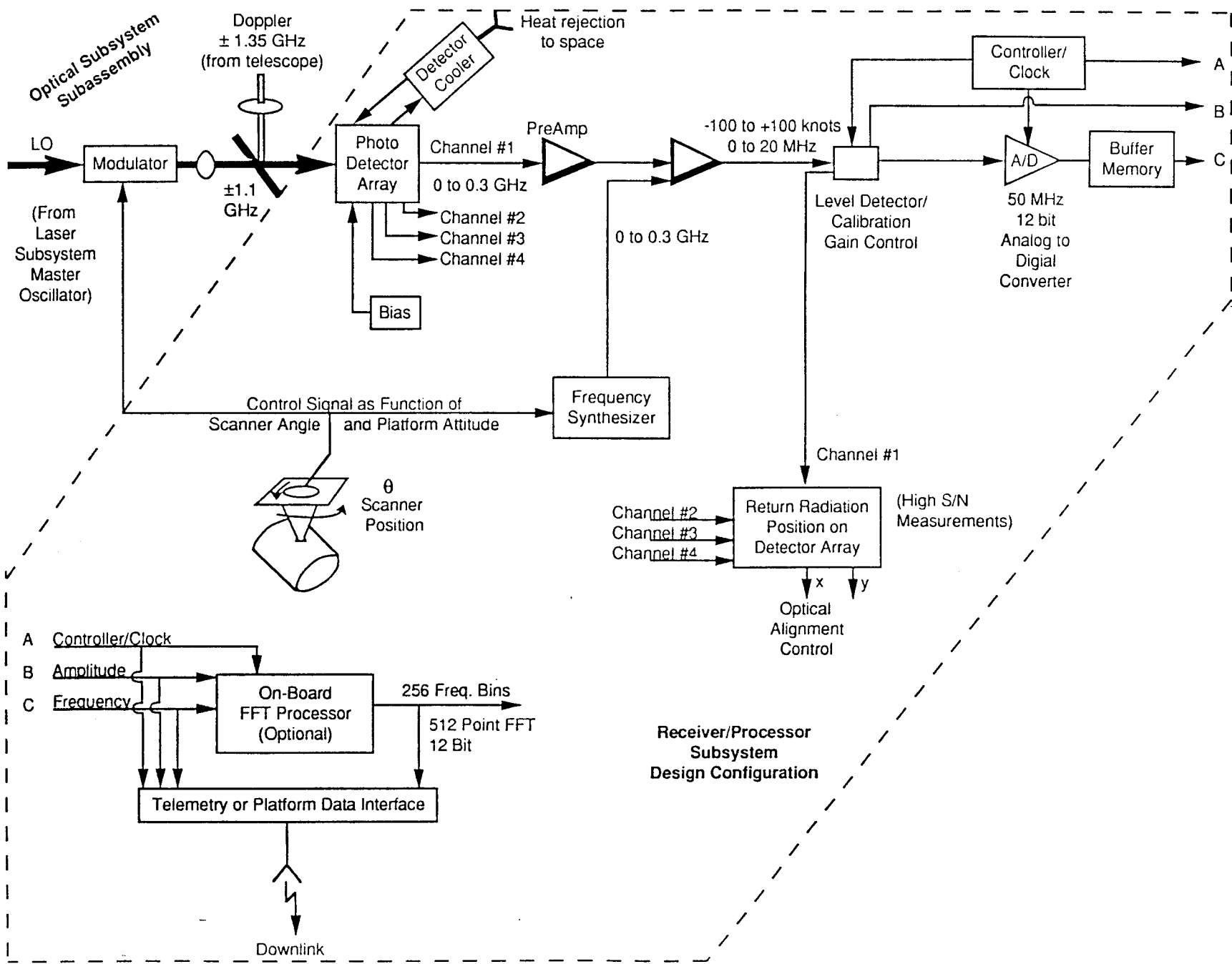


Figure 20. LAWS Receiver/Processor Block Diagram

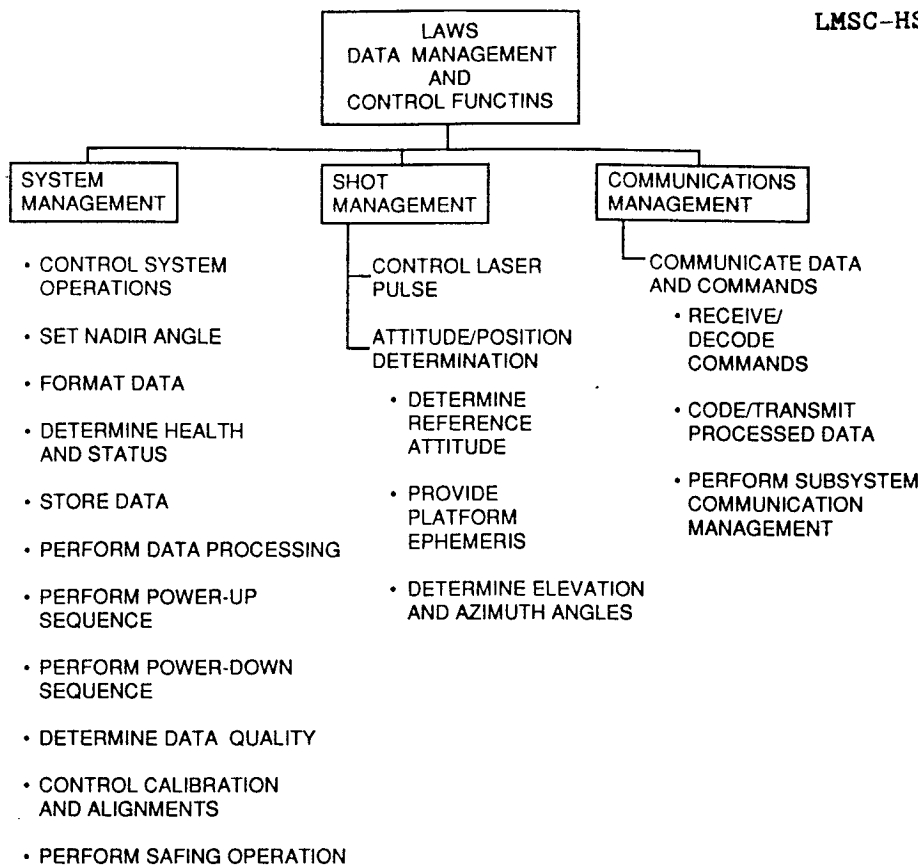


Figure 21. LAWS Flight Data Management Functional Hierarchy

## 2.5 ELECTRICAL POWER SUBSYSTEM

The Electrical Power Subsystem baseline design is summarized below:

- Interfaces with platform prime power and provides circuit protection/filtering to/from prime power source
- Provides power at appropriate level to all subsystems via distribution box, circuit breakers, and shielded cables
- Provides emergency stand-by power
- Controls electromagnetic interference to/from platform via shielding and ground system.

The baseline Electrical Power Subsystem consists of the connectors to platform power, the power distribution box, the circuit protection assembly, the power conditioning assembly, and the power distribution cables. The Electrical Power Subsystem receives power from the platform solar cells/batteries and conditions/distributes the power to other LAWS subsystems with provisions for circuit protection and stand-by emergency power. Circuit protection is designed to prevent catastrophic failure from accidental shorts during assembly and deployment. Circuit protection will protect the LAWS

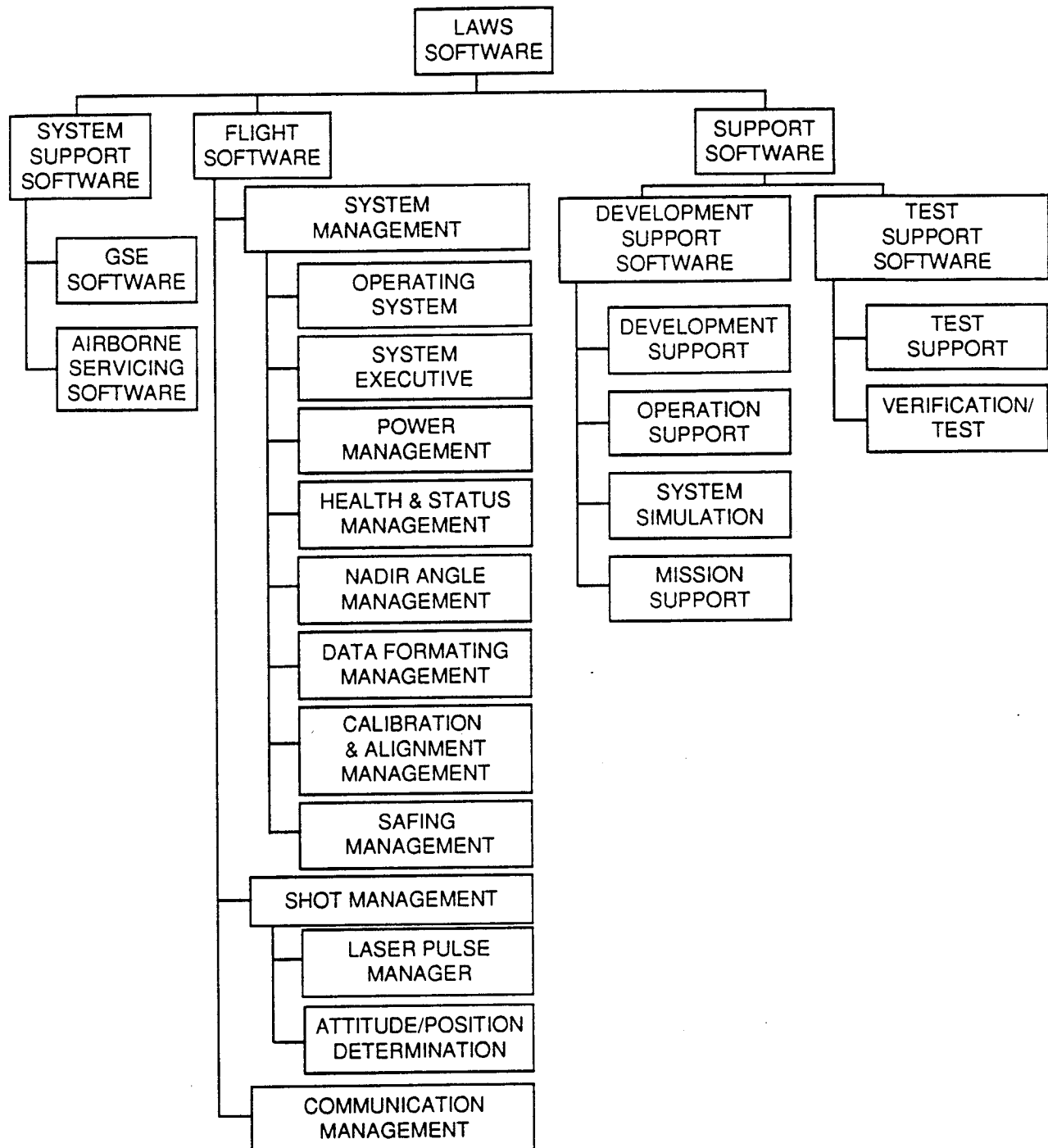


Figure 22. LAWS Software Tree

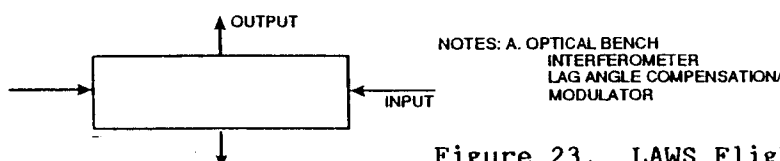
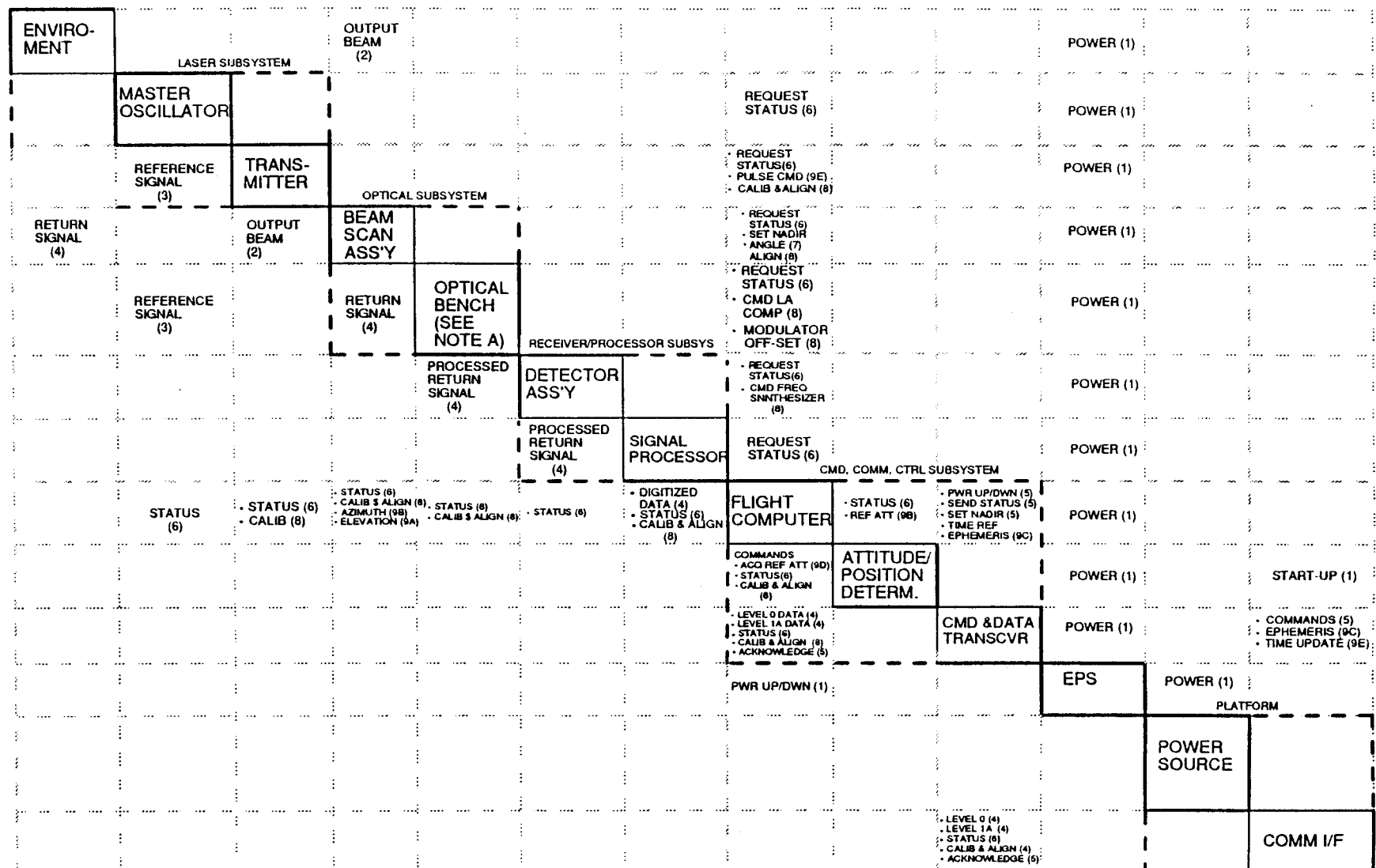


Figure 23. LAWS Flight Software Command and Data Flow Management

Instrument from power surges potentially introduced by faults from other platform payloads and will likewise limit LAWS Instrument effects upon the platform prime power. Emergency power is in the form of stand-by power and heating when subsystem components are in a non-operating mode and prevents freezing of fluids and joints. Charge, discharge, and power utilization cycles are depicted in Figure 24.

## 2.6 MECHANICAL SUPPORT SUBSYSTEM

The mechanical Support Subsystem baseline design is summarized as follows:

- A base platform constructed of structural edge beams with rib stiffened panels, and major structural cross members, serves as the mechanical interface to the space platforms and the launch vehicles
- A grapple fixture for RMS or tele-operator handling (SSF Option)
- A thermal control system with cold plate interface to space platform thermal system or with a space radiator if the platform (JPOP) has no cooling loop available
- A C<sub>18</sub>H<sub>38</sub> phase change wax thermal reservoir to support varying thermal loads due to shot management.

The Mechanical Support Subsystem consists of the base platform to which the LAWS subsystems are attached, the grapple fixture for in-space positioning, attachments for both launch vehicle and/or space platform accommodation, and the thermal control system. Baseline design of the platform is an aluminum skinned structure with aluminum ribs and beams covered with a multi-layer thermal protection system. Detail thermal, optical, and structural analyses will be performed during Phase II to ensure the following:

- Optical misalignment due to structural distortion from thermal and mechanical loads are within system tolerances
- Overall LAWS weight stays within system requirements.

Initial sizing indicates that the aluminum base structure is within the total LAWS weight budget. Composite structures will be investigated in Phase II for weight savings and minimization of structural distortion.

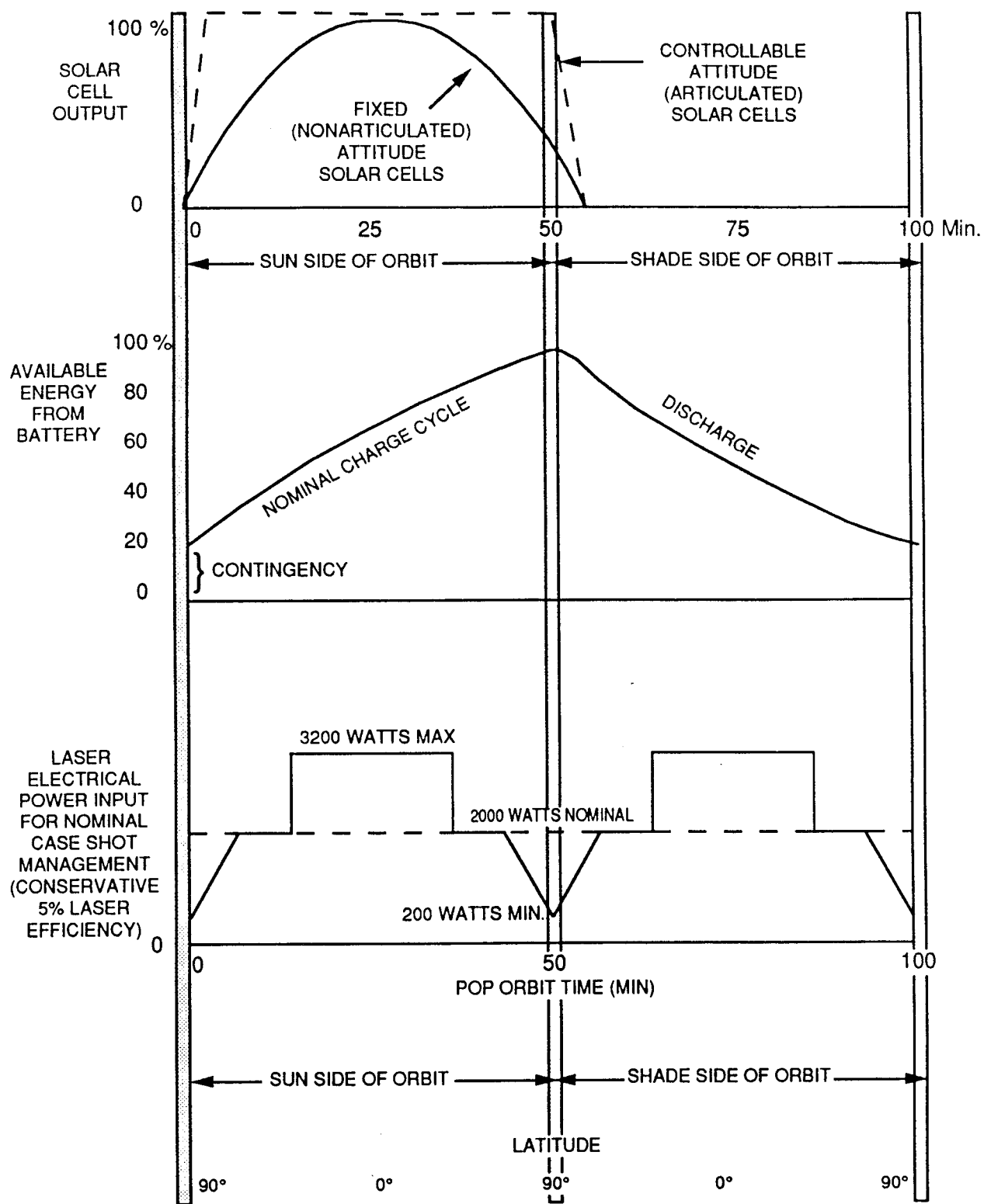


Figure 24. Electrical Parameters as Function of Position in POP Orbit for Typical 100 Minute Orbit

### SECTION 3. PERFORMANCE ANALYSIS

LAWS is designed to monitor global tropospheric wind profiles. Over a significant portion of the globe, LAWS will be operating in regions of low aerosol ( $\beta$ ) concentrations. This results in a relatively weak backscattered radiation return to the Instrument and a low signal-to-noise ratio (SNR) measurement. A number of velocity estimators have been used to examine the expected performance of LAWS as a function of measurement SNR. These estimators include the pulse-pair estimator used with NASA and NOAA coherent lidars on one extreme, to the Cramer-Rao lower bound at the other (with the FFT and Capon estimators falling between these extremes).

These estimators, along with a given platform power constraint, have been used to determine an optimal pulse repetition rate for LAWS. Figure 25 depicts the standard deviation of line-of-sight winds (Sig. R) divided by the square root of the number of pulses (SQR(N)) within the grid for 3200 W laser input power. The 3200 W has been derived as a peak input laser power; averaged over the orbit the average input power becomes  $\leq$  2000 W for the orbital parameters shown and latitude shot management. Figure 25 shows that for a 20 J laser and with the parameters known, 8 Hz is a near optimal pulse repetition rate. If a less ideal estimator such as the pulse pair estimator is used, this function shows a stronger break point at 8 Hz. The less ideal (pulse-pair) estimator also shows a 30 percent improvement in (SIG.R)/SQR(N) for the 20 J/pulse case over the 10 J/pulse case. For the Cramer-Rao lower bound, 20 J/pulse provides an improvement over 10 J/pulse at twice the repetition rate, although the improvement is not as dramatic.

Figures 26 and 27 depict a trade between telescope aperture and laser power for a LAWS Instrument with 400 kg allocated to the combination Optical and Laser Subsystems. As the laser energy output is increased, the laser weight increases; likewise as the telescope aperture increases, the telescope mass increases. The relationships between telescope aperture and mass and laser energy and mass (Figure 27) were derived at the Concept Review. As Figure 26 shows, performance begins to level off at 20 J/pulse and peaks at 30 J/pulse. Risks also increase with laser energy/pulse, and 20 J/pulse has been selected as an optimal risk/performance point for our LAWS concept. We are confident that we can develop the 20 J/pulse laser and would be much more concerned about risks associated with a 30 J/pulse laser. We are also confident of our capability to field a 1.67 m aperture telescope to meet LAWS weight requirements.

Figure 28 depicts measured SNR as a function of global coverage for data at the 10 km altitude for orbital altitudes of 400, 500, 600, 700, and 800 km and off-Nadir scan angles of 30, 40, 50, and 60 deg. From this figure it can be seen that a 35 deg angle and 700 km orbit will provide approximately 40 percent global coverage with 10 dB SNR at the 10 km altitude, while with a 55 deg angle it will provide almost 80 percent coverage with 6 dB SNR.

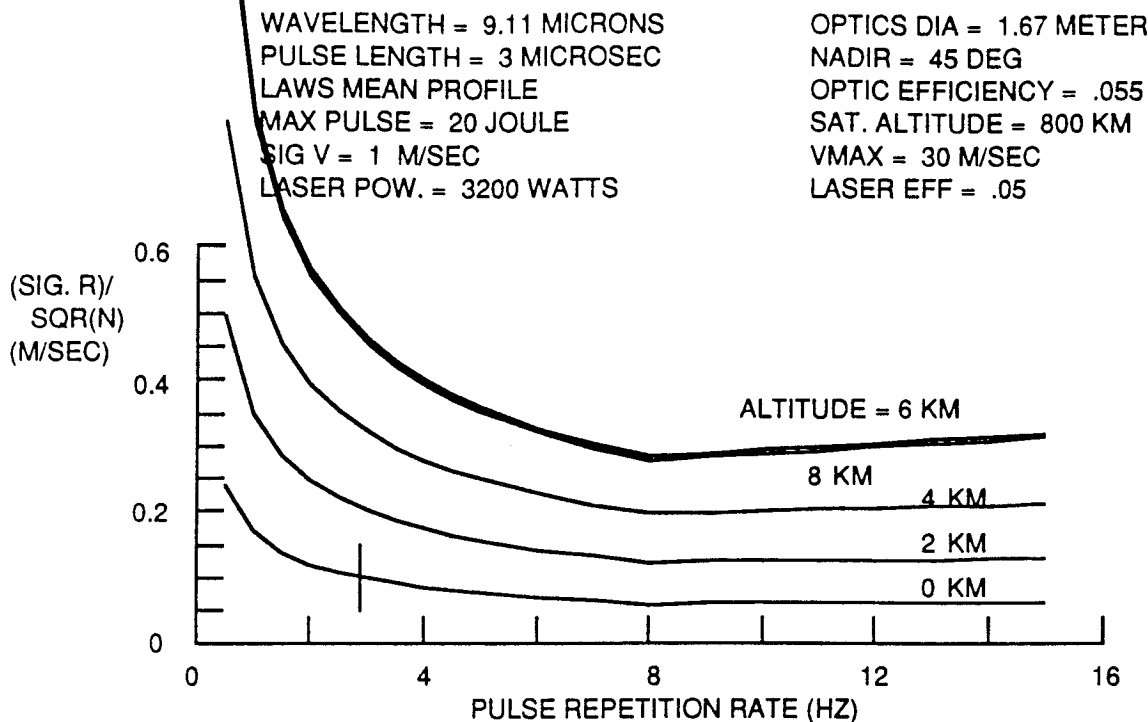


Figure 25. Optimal Allocation of Power for 20 J Maximum Laser Pulse Energy (Cramer-Rao Estimator)

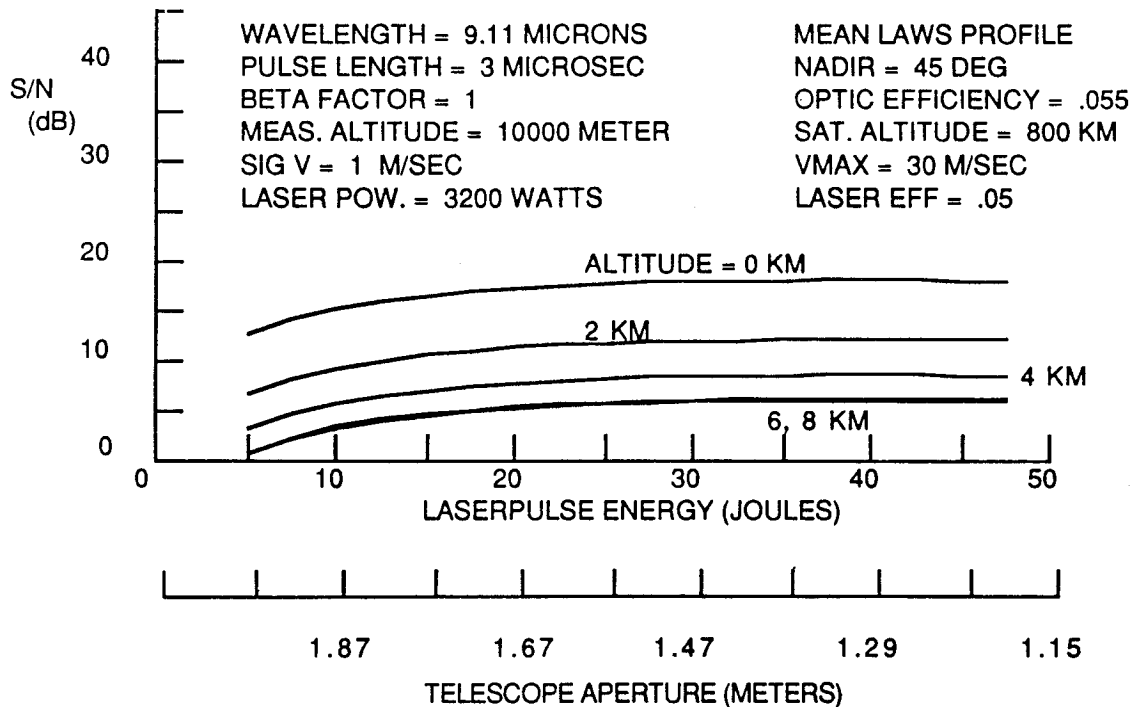


Figure 26. Optimal Allocation of Weight for a 400 kg Sum of Laser Mass and Telescope Mass

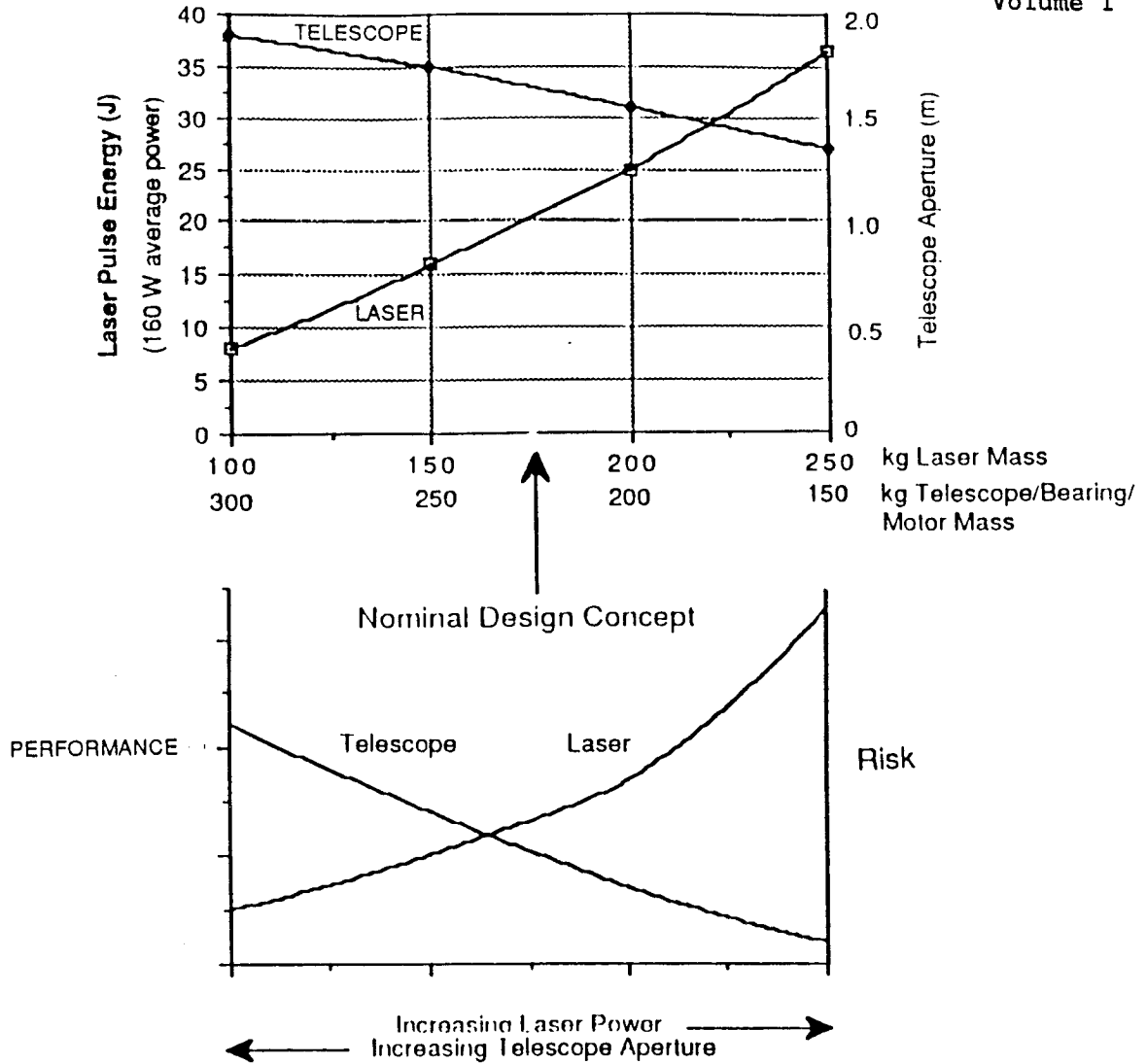


Figure 27. 400 kg Combined Laser/Telescope/Motor/Bearing Concept Trades

Figure 29 depicts our recommended azimuth controlled (shot management) pulsing scheme with the majority of the shots placed near where intersecting (line-of-sight) vectors can be measured. Two average power repetition rates are depicted in the figure: one with a laser input of up to 3200 W (8 Hz average laser output at 20 J/pulse) and one with average input of 2000 W (5 Hz average output at 20 J/pulse). The 8 Hz average rate will be used between the equator and 30 deg latitude where the rate will drop to 5 Hz (between 30 and 50 deg). Between 50 deg and the poles (90 deg), the rate will gradually drop to near-zero. Our laser design calls for "shoot upon demand," allowing considerable flexibility for shot management during each quarter of orbit. Both our electrical power and thermal management schemes are designed to handle non-linear loads created by this shot management scheme. Figure 30 depicts two LAWS polar orbits with the swaths overlapping above 52 deg north latitude. If uniform global coverage is desired, this figure illustrates the requirement for shot suppression in regions near the poles.

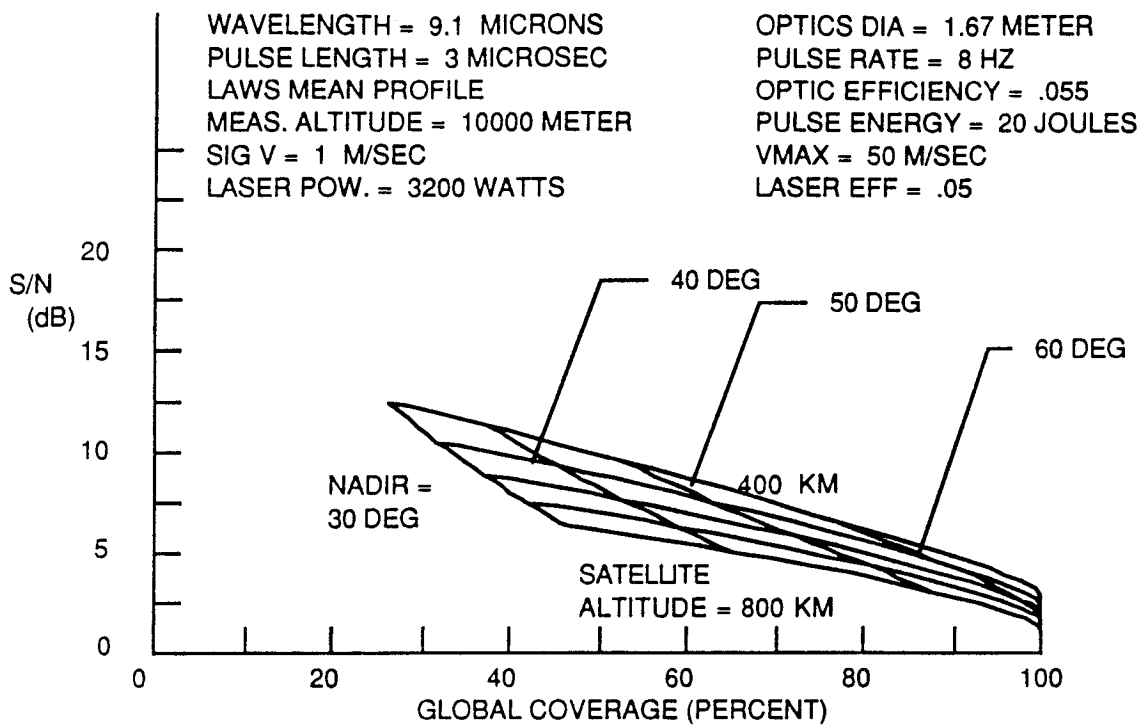


Figure 28. Trade of Global Coverage vs Data Quality as Expressed by SNR for Low Backscatter (High Altitude)

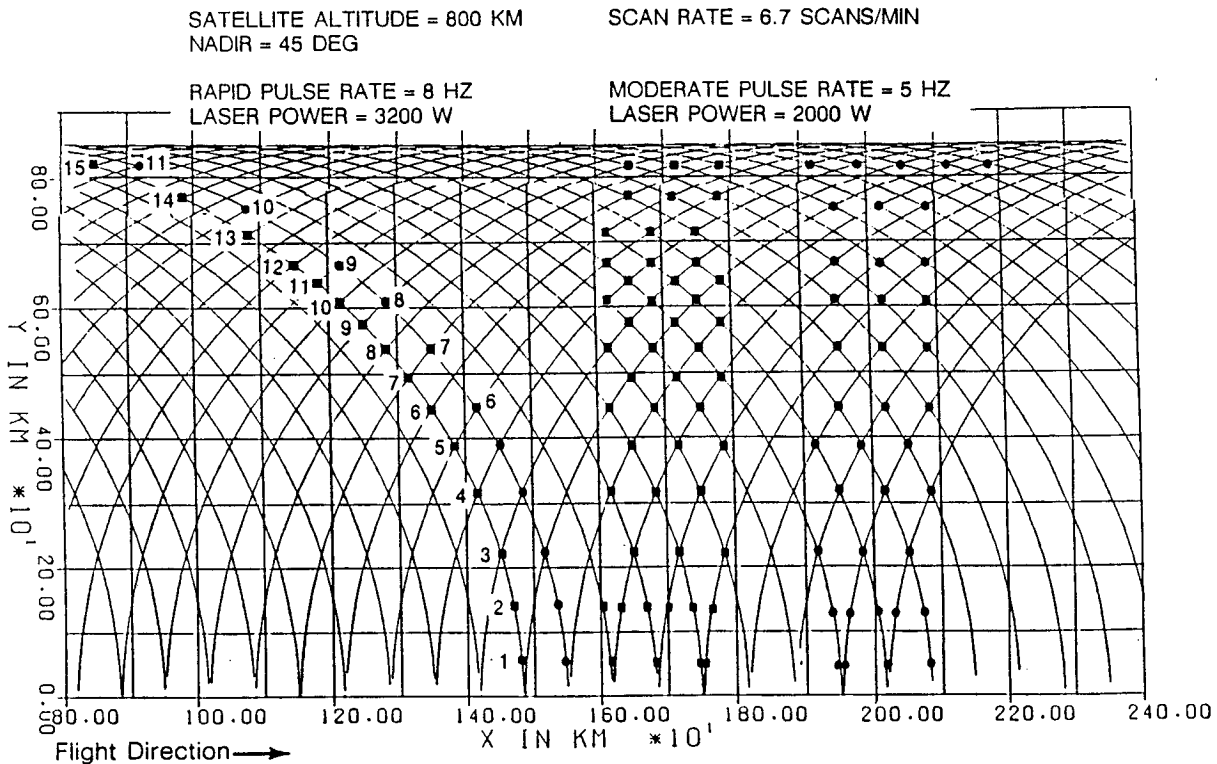


Figure 29. Azimuth Controlled Pulsing

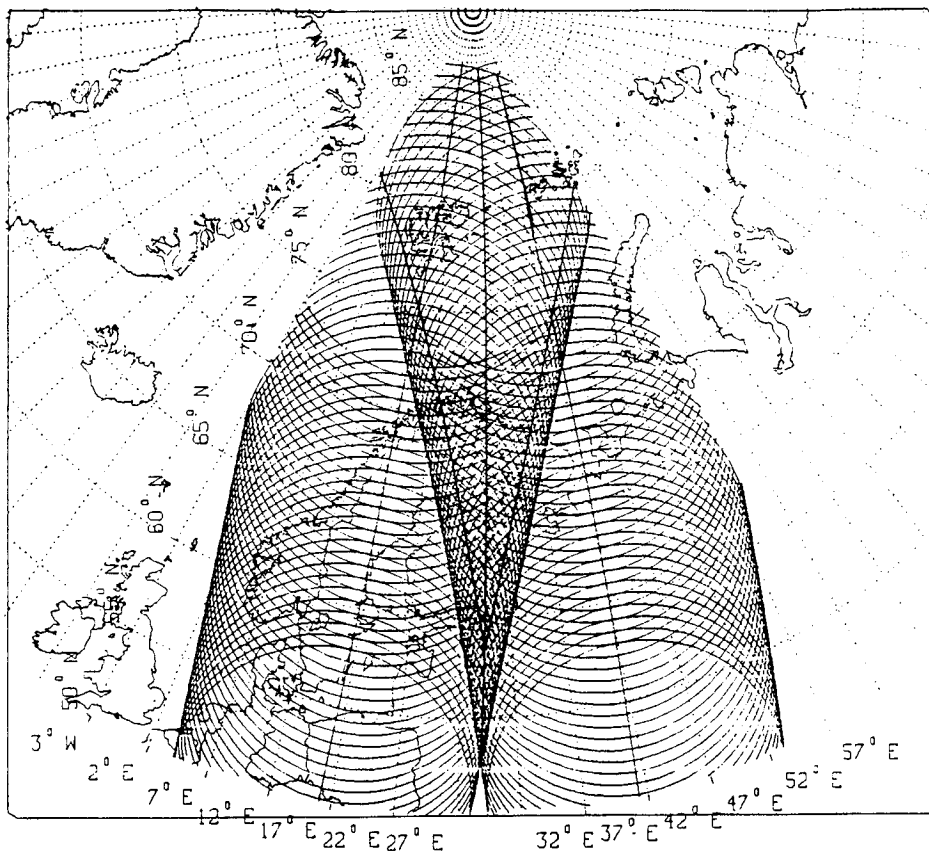


Figure 30. Scanning and Latitude Shot Management

A computer simulation developed under a Lockheed IRAD program was used to model the LAWS lidar. Examples from cases with specified pulse lengths and processing window lengths are depicted in Figures 31 and 32. Figure 31 depicts a wind field with simulated velocity gradient reversals every km, and Figure 32 depicts a continuously varying wind field. The plots on the left in each figure describe the modeled wind field, and the plots on the right statistically depict the measurement error, i.e., percentage of data points with errors of less than 1 m/sec using the FFT estimation. In both figures, the simulated transmitted pulse was 1.6  $\mu$ sec; and the receiver windows were matched in the top figures, twice as long as the pulse in the center figures and four times as long in the lower figures. For the constantly varying wind field, the percentage of points within 1 m/sec improves with each increase of window length. However, for the zig-zag wind field, doubling the processing window (from matched to 2X the pulse length) improved the error statistics. Yet doubling the window again (to 4x the pulse length) degraded the statistics because the window overlapped reversals of the wind field. Operation of this simulation with modeled LAWS data has provided insight into requirements for the LAWS Instrument.

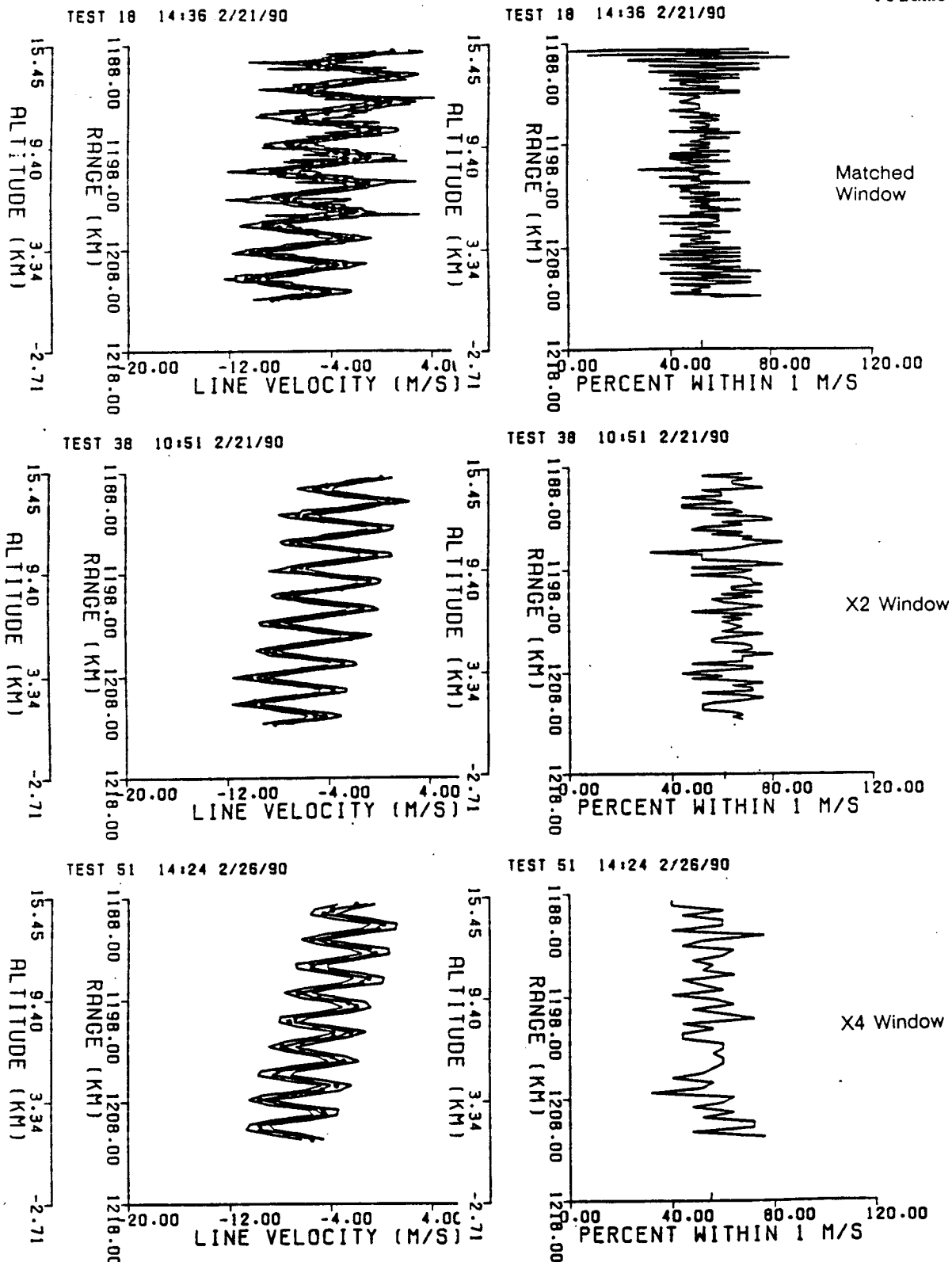


Figure 31. Short Pulse (1.6  $\mu$ sec) and Window Lengths of 32 (Matched), 64 (x2), and 128 (x4) Samples (Wind field with velocity gradient reversals every 1 km)

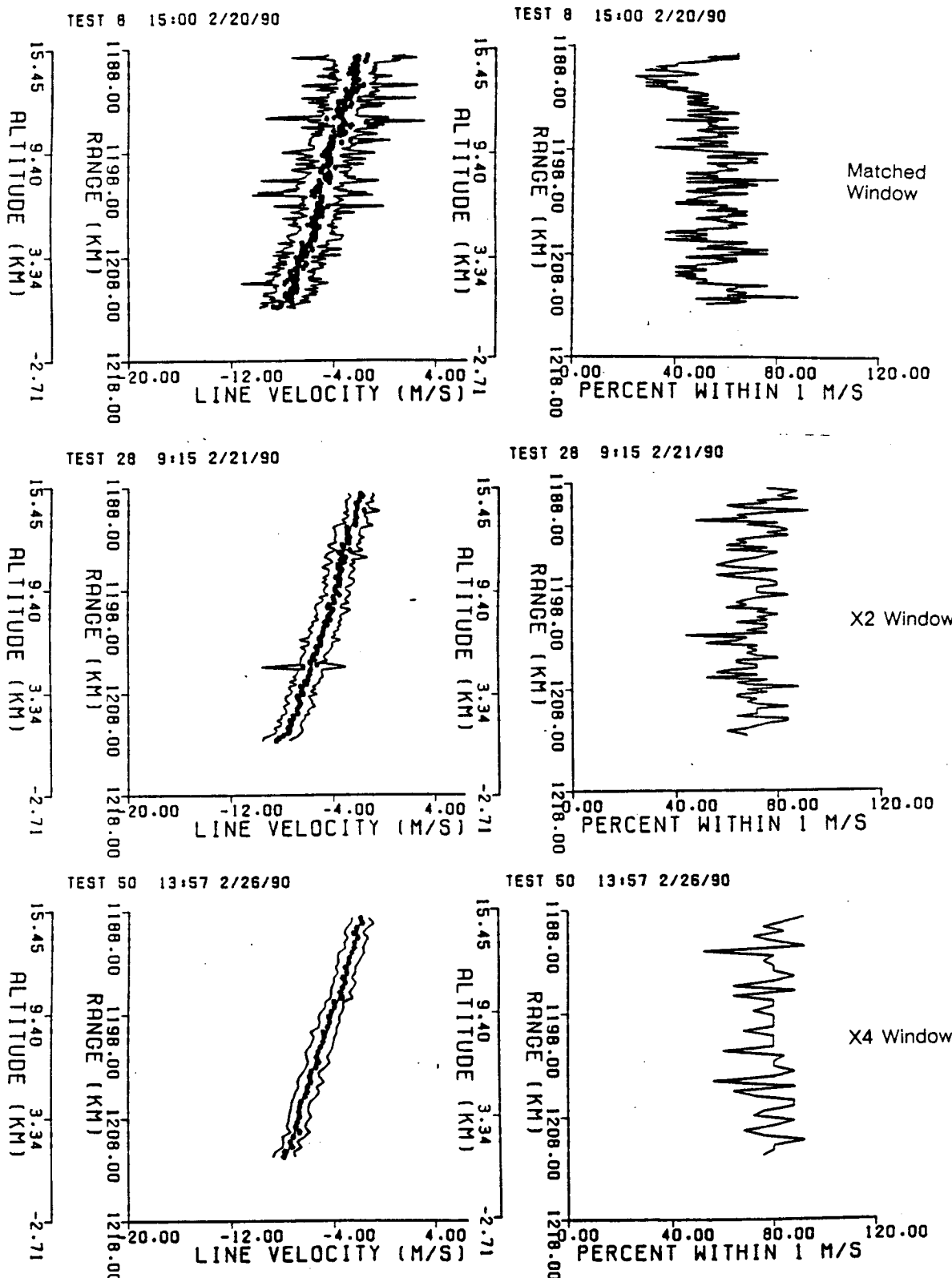


Figure 32. Short Pulse (1.6  $\mu$ sec) and Window Lengths of 32 (Matched), 64 (x2), and 128 (x4) (Continuously Varying Wind Field)

#### SECTION 4. LAWS BASELINE CONFIGURATION AND ACCOMMODATION

The integrated LAWS Baseline configuration is shown in Figure 33. This baseline concept easily accommodates either the Avco or GEC laser design. All components can be packaged within an area approximately 2 m by 2 m on the aft end of the base structure, leaving the forward area clear for the telescope. The tapered, contoured telescope yoke design provides for a minimum rotation envelope to facilitate this compact layout. The grapple fixture is included to assist in on-orbit servicing and positioning utilizing the RMS or tele-operator systems. All RMS clearance envelopes required for the grapple fixture are accommodated. The baseline configuration is contained in a maximum volume of 3.94 m x 2 m x 2.31 m.

The telescope is constrained with its axis parallel to the base structure by the yoke and a forward attach point for launch load environments. Once on-orbit in the operational mode, the telescope rotates about the yoke pivot points to the desired off-nadir viewing angle and can sweep through the full 360 deg field of view as shown in Figure 34.

The baseline configuration's mass, volume, c.g., and power characteristics are presented in Table 2. All parameters are seen to be well below the specified budgets. A detailed breakdown for the LAWS/GEC laser configuration is shown in Table 3. Due to lack of design and interface data for the Japanese Polar Orbiting Platform (JPOP), a LAWS self-contained thermal control system with panel radiator was developed as an option to the baseline configuration, shown in Figure 35. This radiator has a planform area of 4.8 m<sup>2</sup> and is positioned, when deployed, with edges perpendicular to earth and sun and both sides viewing deep space. Total exposed radiation area is 9.6 m<sup>2</sup>, sufficient to maintain all LAWS subsystems within their normal operating temperatures. The radiator attaches to the telescope yoke and base structure for launch environment, and pivots and rotates to position on-orbit.

The Lockheed LAWS configuration is designed to accommodate installation on polar orbiting platforms (shown in Figure 34) and/or SSF (shown in Figure 36). Space Station installation is directly to the payload interface adapter (PIA), mounted on the station interface adapter (SIA). The LAWS thermal control system will interface with the station thermal control system cold plate on the PIA. This will delete the requirement for the LAWS radiator from the configuration, providing a 68 kg weight reduction. The LAWS interface structure that mates with the PIA can be biased to compensate for the negative pitch angle of the operational SSF, dependent on final station design. Launch to orbit can be by the Space Shuttle (STS) shown in Figure 37, or unmanned expendable launch vehicles such as H-II or Titan.

Figure 38 shows the POP/LAWS configuration in the 3.65 m diameter fairing for the Japanese H-II launch vehicle. The base end of the POP would interface with the boost vehicle for launch/flight load reaction. Similar configuration

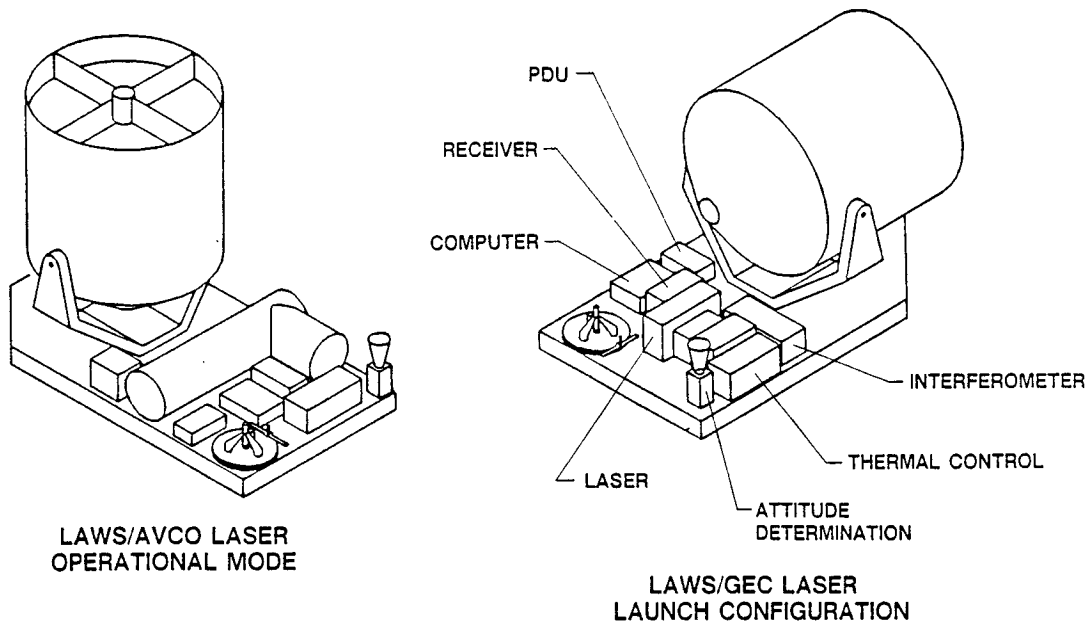


Figure 33. LAWS Baseline Configurations

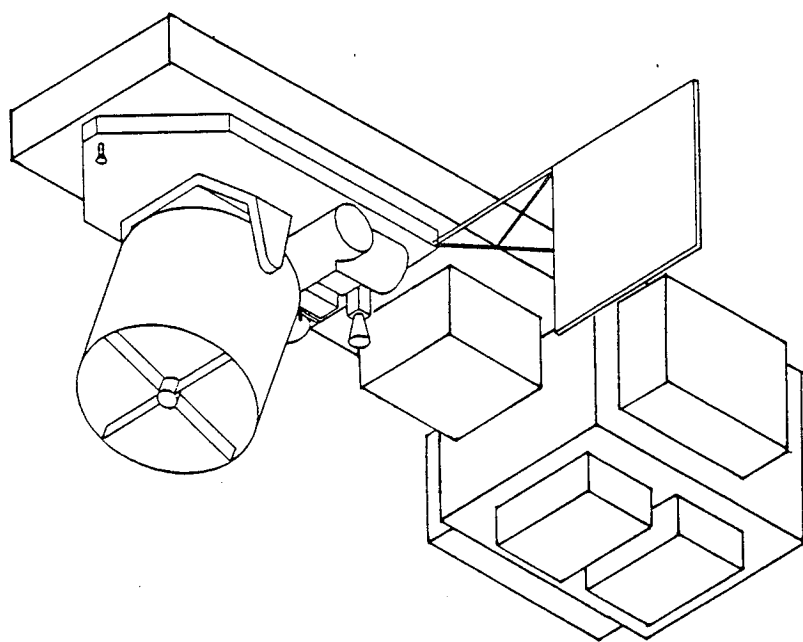


Figure 34. Typical LAWS/POP Configuration

Table 2. LAWS BASELINE PARAMETERS

Configuration	Weight (kg)	Envelope Dimensions (m)	Power (watts)	Data Communication Rate	Thermal Control Requirement (watts)
Budget	800	Accommodate H-II/Titan ELVs and Space Shuttle (STS)	3000 Avg. (4200 Peak with Shot Management)	Compatible with TDRSS	Space Bus Compatibility or Integral System
LAWS/AVCO Laser	763	3.9 x 2 x 2.31	3323 (Peak)	Temporary Data Storage for Transfer to Platform/TDRSS	2922
LAWS/GEC Laser	743	3.5 x 2 x 2.31	3227 (Peak)	Temporary Data Storage for Transfer to Platform/TDRSS	2088

LAWS 3-1

Table 3. BASELINE CONFIGURATION/GEC LASER

Item	Weight (kg)	X	CG Location (M)	Y	Z	Power Required (watts)	Active Thermal Control Requirement (watts)
Optical Telescope	93	+1.20	0.0	0.0	0.0		Internal In System
Yoke/Gimbal Mechanism	85	+0.24	0.0	0.0	0.0	221	
Interferometer	45	.12	.56	-.85			
Laser	167	.20	.20	-1.32	2716 (Peak)	1818	
Flight Computer	18	.07	-.72	-1.08	20	20	
Attitude Determination System	8	.09	.84	-1.90			
Power Distribution Unit	13	.07	-.68	-0.58	20	-	
Receiver	10	.13	-.34	-1.08	50	50	
Grapple Fixture	13	.04	-.70	-1.80	-	-	
Base Structure	205	-.10	0.0	-.37	-	-	
Radiator w/Support Structure	68	.65	+1.0	-.67	-	-	
Thermal Control Total System	18 743 kg	.14 .27M	.84 .15M	-1.44 -.65M	200 3227 (Peak)	200 2088	

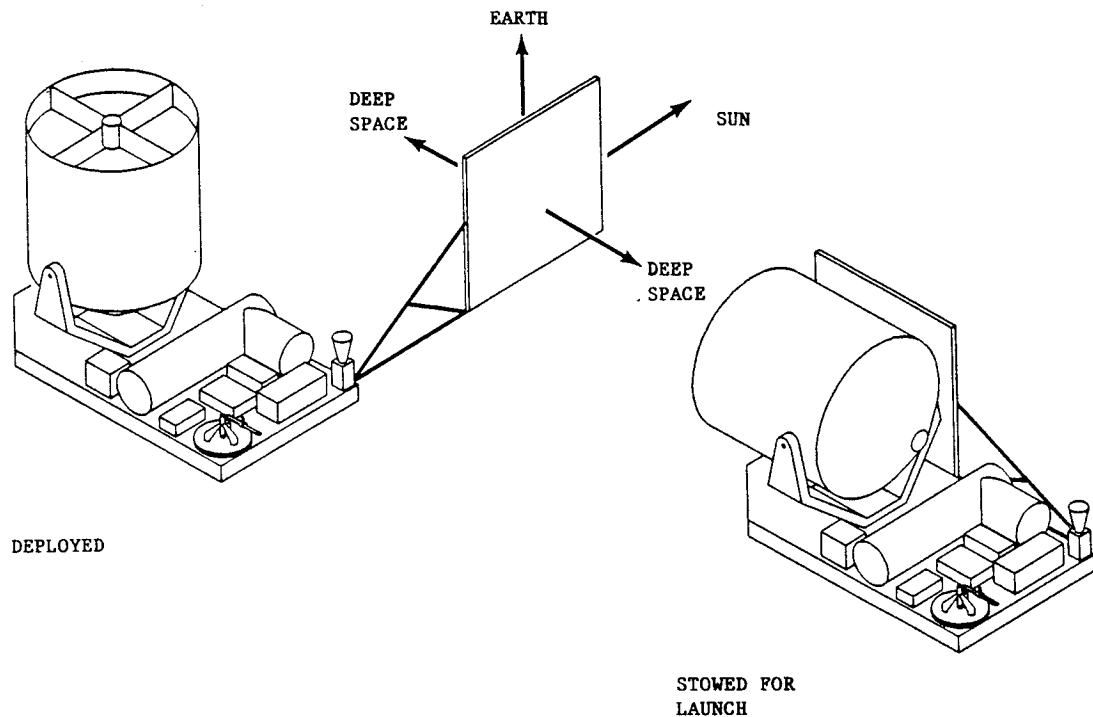


Figure 35. LAWS with Radiator

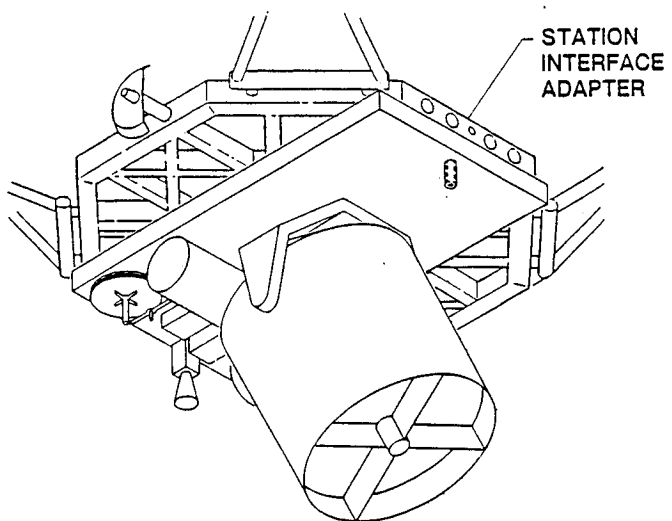


Figure 36. Space Station Installation

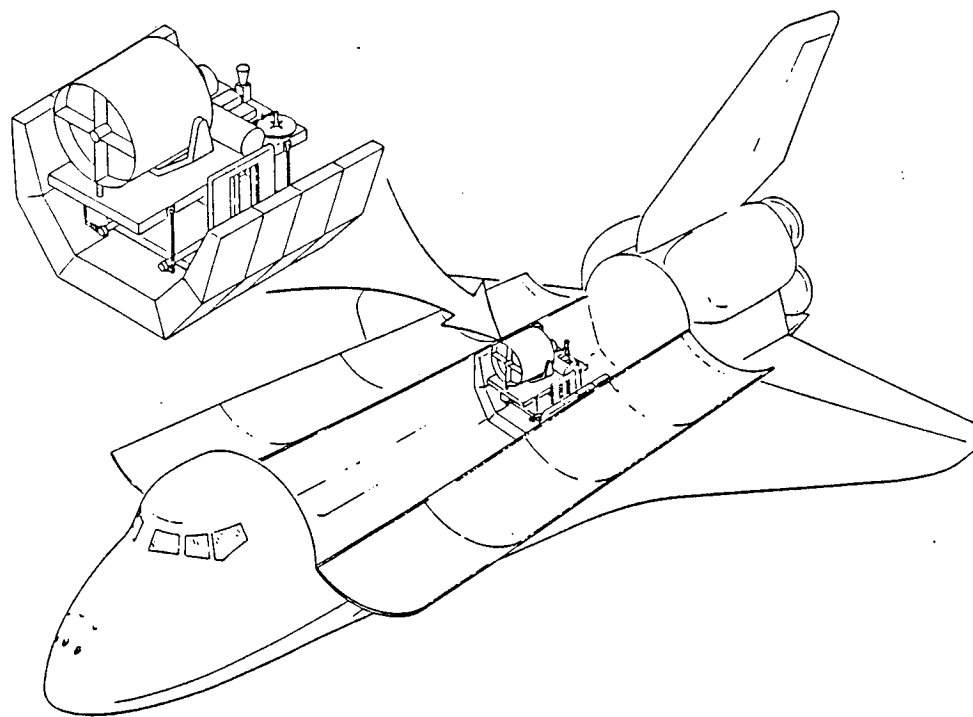


Figure 37. Shuttle Launch Configuration

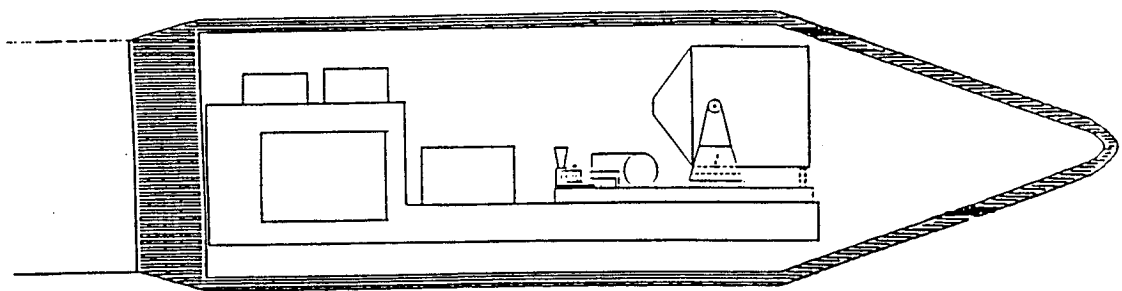


Figure 38. H-II Launch Configuration

would be used for the Titan launch vehicle. The STS/LAWS launch configuration shown in Figure 37 would utilize the Hubble Space Telescope Orbital Replacement Unit (ORU) Carrier design developed for the HST maintenance and refurbishment missions. This ORU carrier is based on a standard Spacelab pallet and was designed by MSFC and fabricated/assembled/verified by Lockheed-Huntsville. The HST ORU carrier system was space flight qualified for maximum payloads up to 1451 kg, well above our maximum LAWS weight of 763 kg. LAWS would be removed from the ORU carrier/STS cargo bay by the RMS, using the LAWS grapple fixture for transfer to the Space Station SIA.

Servicing can be performed at the SSF by astronauts during EVA. All components except the telescope can be replaced on-orbit using standard NASA inventory EVA tools. These change-out procedures have been developed and validated through many hours of 1-g and neutral buoyancy simulations on Lockheed's HST, AXAF, and SSF contracts and development work. There will be no orbital servicing with JPOP.

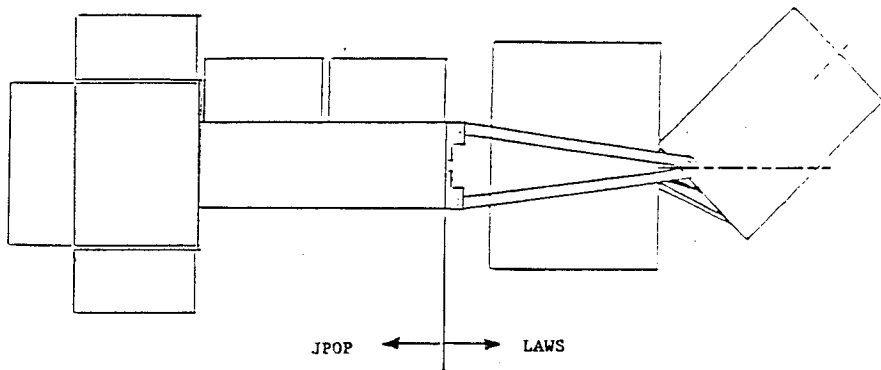
#### 4.1 ALTERNATE LAWS CONFIGURATION

Due to the uncertainty in the configuration concept of the polar orbiting platform, particularly the JPOP, an alternate LAWS configuration was developed. This configuration will accommodate installation on a preliminary JPOP concept (Figure 39) shown by NASDA during the August 1989 LAWS Quarterly Review. This LAWS configuration, with either the Avco or GEC laser (shown in Figure 40), will accommodate installation on JPOP and/or the SSF and launch by STS or unmanned vehicles.

On JPOP, the alternate LAWS would mount directly to the front end of the vehicle shown in Figure 41, and the JPOP vehicle would also provide the structural mount for H-II or Titan launch, shown in Figure 42.

For Space Station installation, the Alternate LAWS would interface with the station PIA/SIA through a Deck Carrier Assembly structure, as shown in Figure 43. The Deck Carrier Assembly would also be used as the interface structure for STS launch as shown in Figure 44. Table 4 gives a detailed weight breakdown for the alternate LAWS configuration with the Avco laser.

Alternate LAWS weight is approximately 80 kg less than the baseline LAWS due to the reduction in base structure weight and more compact packaging.



PRELIMINARY CONCEPTS

- Telescope restricted to arc survey sweep
- Gravity gradient mode necessary for full 360 conical survey



Figure 39. Preliminary JPOP/LAWS

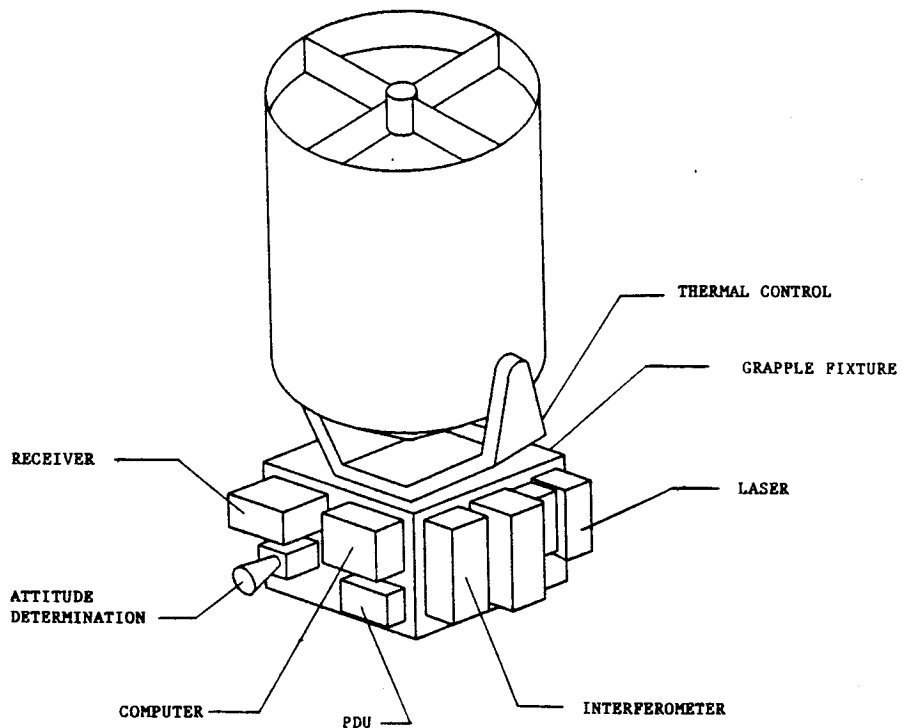


Figure 40. Alternate LAWS Configuration

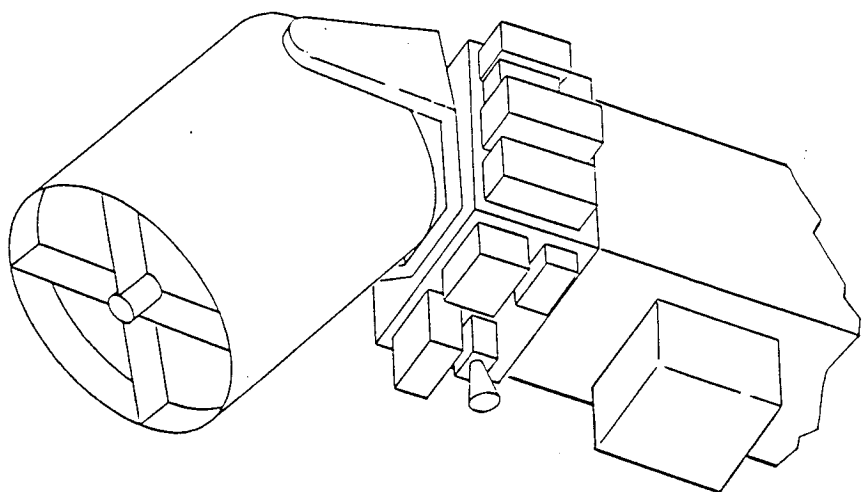


Figure 41. JPOP Installation

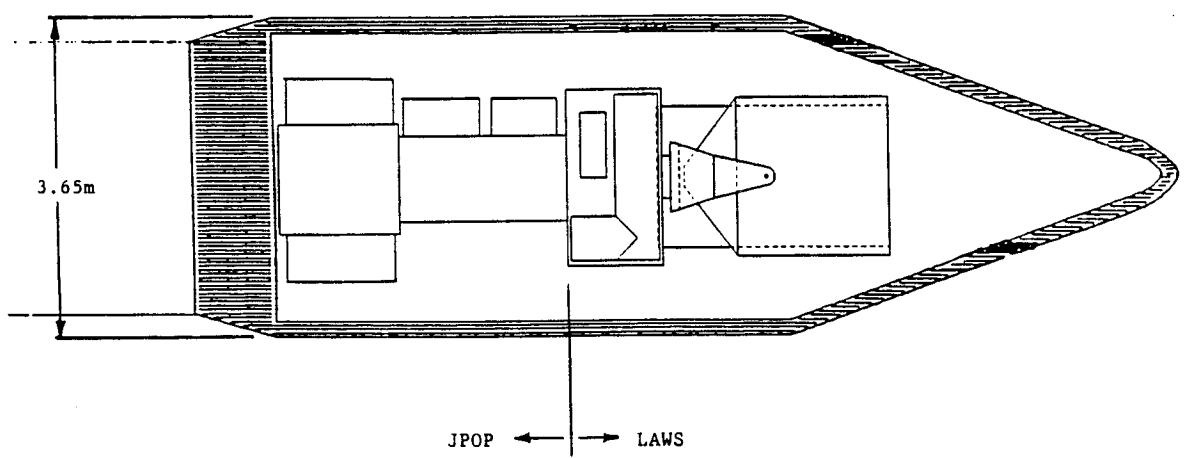


Figure 42. H-II Launch Configuration

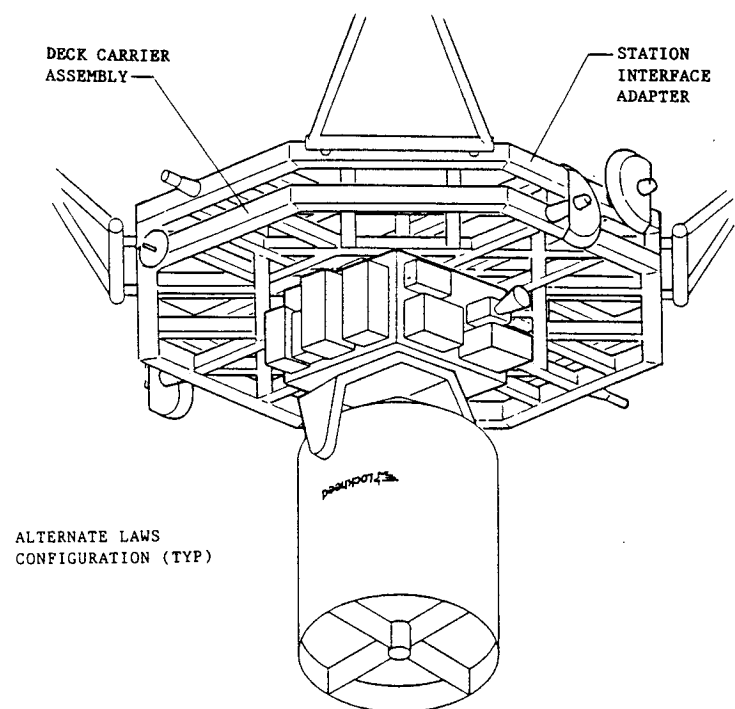


Figure 43. Space Station Installation

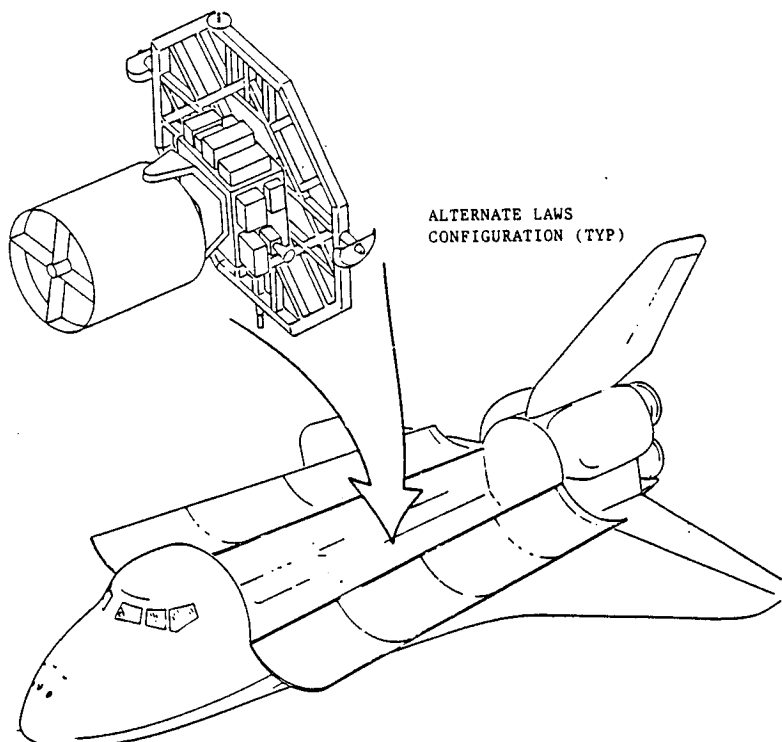


Figure 44. Shuttle Launch Configuration

Table 4. ALTERNATE CONFIGURATION/AVCO LASER

<u>Item</u>	<u>Weight (kg)</u>	CG Location (M)		
		X	Y	Z
Optical	93	+1.20	0.0	0.0
Yoke/Gimbal Mechanism	101	+0.10	0.0	0.0
Interferometer	45	-.80	-.40	-.74
Laser	171	-.43	.23	-.88
Flight Computer	18	-.35	-.67	+.40
Power Distribution Unit	13	-.84	-.56	+.68
Receiver	10	-.35	-.56	+.80
Attitude Determination	8	-.54	+1.03	-.22
Grapple Fixture	13	-.80	-.92	-.32
Radiator w/Support Structure	61	+.44	0.0	+.123
Base Structure	128	-.55	0.0	+.04
Thermal Control	<u>18</u>	<u>-.74</u>	<u>.65</u>	<u>+.55</u>
Total System	679 kg	-.13M	-.03M	-.17M

## SECTION 5. PROJECT COST ESTIMATES

The LAWS cost modeling activities were initiated in Phase I to establish the ground rules and cost model that would apply to both Phase I and Phase II cost analyses. The primary emphasis in Phase I has been development of a cost model for a LAWS Instrument for the JPOP. However, the Space Station application has also been addressed in this model; elements have been included, where necessary, to account for Space Station unique items. The cost model presented in the following sections defines the framework for all LAWS cost modeling. The model is consistent with currently available detail, and can be extended to account for greater detail as the project definition progresses.

This section discusses the estimating methodology used in the LAWS Phase I studies, identifies the Work Breakdown Structure (WBS) elements to which costs will be allocated, and identifies the Cost Estimating Relationships (CERs), and other cost factors used to determine the LAWS Phase C/D estimated costs.

### 5.1 COST ESTIMATING METHODOLOGY

Estimation of project cost is an evolutionary process. In the early project definition stages (e.g., the LAWS Phase I), there are uncertainties in the estimated cost because neither the hardware nor the programatics (e.g., documentation deliverables, tasks, etc.) are completely defined. An integral part of the cost estimating process is, therefore, to reduce the uncertainties as the system definition matures. Cost modeling and analysis progress from the use of parametric and "similar to" studies in the early stages of a program to a detailed "bottom-up" analysis as the project definition nears maturity.

Parametric pricing is a methodology used when little precise definition is known about the project elements (i.e., hardware, software, tasks, etc.). The methodology is based on the concept of being able to estimate the cost of a new item by correlating its known characteristics to existing items with similar characteristics. This methodology is employed in the LAWS Phase I studies. The parameteric pricing tool used was the RCA-PRICE family of cost models.

Assumptions and Ground Rules. For the LAWS cost estimating studies, two assumptions have been made. First, the JPOP instrument is the baseline design. Second, the Space Station instrument will be adapted from the JPOP design, with specific requirements incorporated into this design.

The LAWS cost estimating studies adopted the following ground rules:

1. All costs are estimated in calendar year 1989 dollars
2. Costs are allocated by WBS elements identified in DR-5, "Draft WBS and WBS Dictionary"
3. The LAWS Instrument development for the JPOP and Space Station platforms is accomplished in a sequential manner
4. There will be no orbital servicing of the JPOP
5. Estimated costs will be audited against historical data at appropriate stages in the LAWS project definition
6. Schedule and budget will be added where technical risk is incurred and development is needed
7. All project burdens (i.e., fees etc.) are assumed to be 15 percent of the total project costs.

These assumptions and ground rules apply for both Phase I and Phase II analyses. The RCA-PRICE model is based on a large historical data base for generically similar items.

## 5.2 LAWS PROJECT WBS ELEMENTS

A draft WBS and WBS Dictionary for the LAWS Phase C/D project is presented in DR-5, "Draft WBS and WBS Dictionary." The elements of that WBS are presented in Figure 45. The WBS Dictionary defines the tasks to be accomplished and thus indicates the allocation of project costs. Tasks associated with these elements are defined to produce the following deliverables:

- One assembled and verified LAWS Instrument flight article
- Data
- Spares
- Systems support equipment
- Software end items.

The WBS presented in Figure 45 is end item oriented for the hardware and software to be produced and services to be performed (e.g., project management, systems engineering, etc.) in producing the end items and for the data to be submitted to NASA-MSFC during the Phase C/D contract activities. It was prepared to Level II, except for software development and orbital servicing task descriptions. The Software Development WBS Element (2.3.2) has been extended to Level IV to clearly delineate separate end items for the software. These are flight, ground, mission, and simulation software end items. The orbital servicing tasks encompassed in WBS element 2.8 comply with the requirement of the LAWS SOW, dated 15 March 1988 for servicing and maintenance

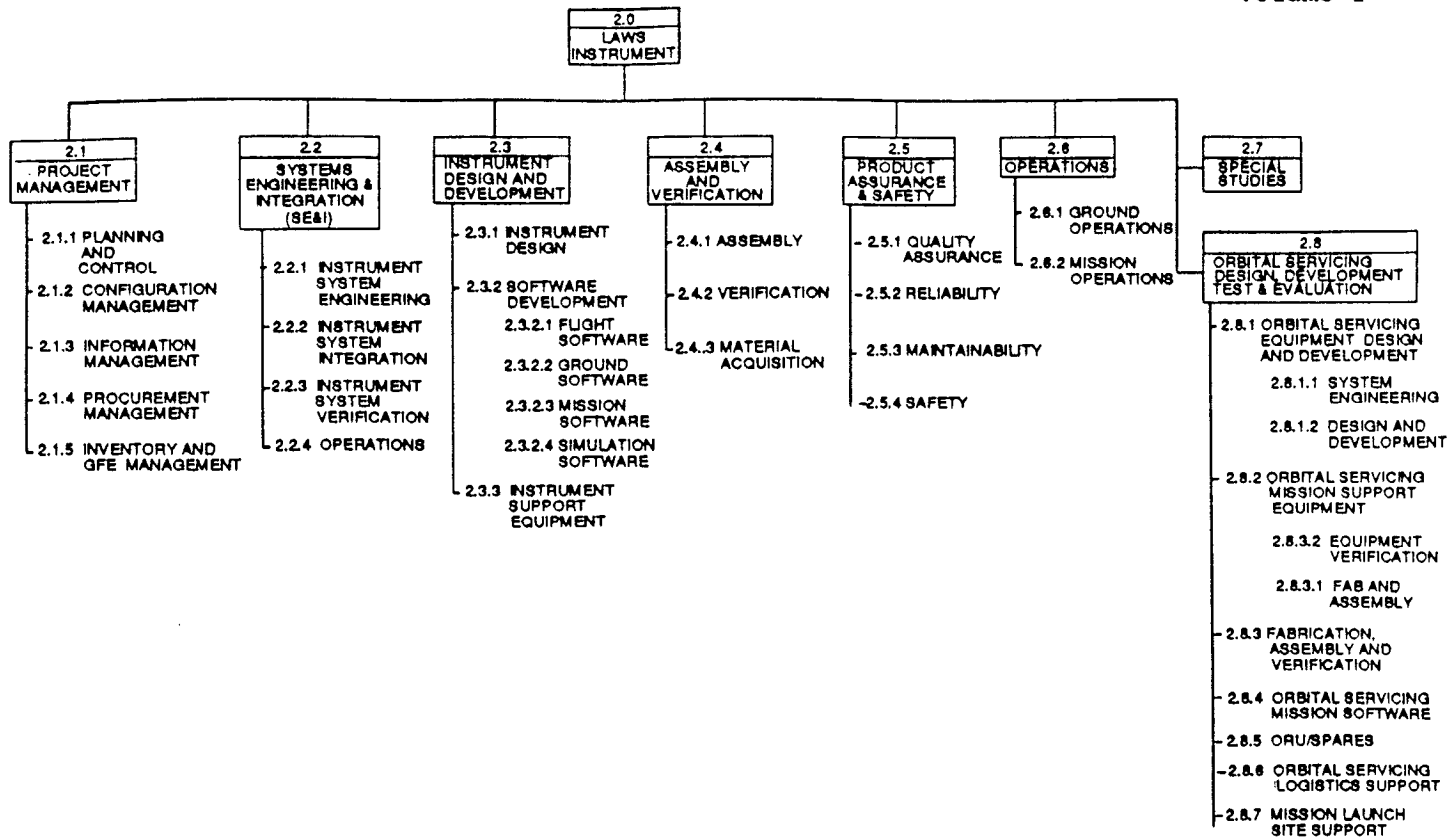


Figure 45. LAWS Project Work Breakdown Structure

of the LAWS Instrument on both the JPOP and the Space Station. Orbital servicing tasks have been extended to Level IV to delineate the various elements required to develop the mission servicing equipment and verify the orbital procedures and/or the equipment developed for servicing the LAWS Instrument.

It is important to note that the RCA-Price cost model allocates costs to systems, data, design, and drafting for hardware items. The manufacturing costs include the material, labor to fabricate, and quality control for the item.

For the purposes of the Phase I analyses, it has been assumed that all subsystems are procured. Therefore, the costs allocated to WBS Elements 2.1, 2.2, 2.3, 2.5, and 2.6 are the prime contractor's costs associated with the LAWS Phase C/D systems engineering, development, product assurance, and operations. All hardware acquisition costs are allocated to WBS Element 2.4. Therefore, this element includes the costs for system integration and verification as well as the hardware.

Cost Model Elements. The primary cost elements for both the JPOP and the Space Station applications are

- Design and development
- Launch vehicle integration and support
- Flight operations and support.

These elements are illustrated in Figure 46 and apply to development of both the JPOP and the Space Station. Design and development include all costs required to design, fabricate, verify, and plan for the flight hardware and system support equipment, and the cost to provide all software. The LAWS Instrument flight hardware consists of the following six subsystems:

1. Laser
2. Optical
3. Command, Communication, and Control
4. Receiver/Processor
5. Electrical Power Distribution
6. Mechanical Support Structure.

Each subsystem is further divided into the assemblies and components identified in Figure 47. There is also a subelement labeled "other" in each subsystem which accounts for additional items that may later be added to that subsystem as the design synthesis matures. The basis for the subelement "other" is a distribution of the system weight contingency. For the current analysis, a cost has been assigned to each item labeled "other."

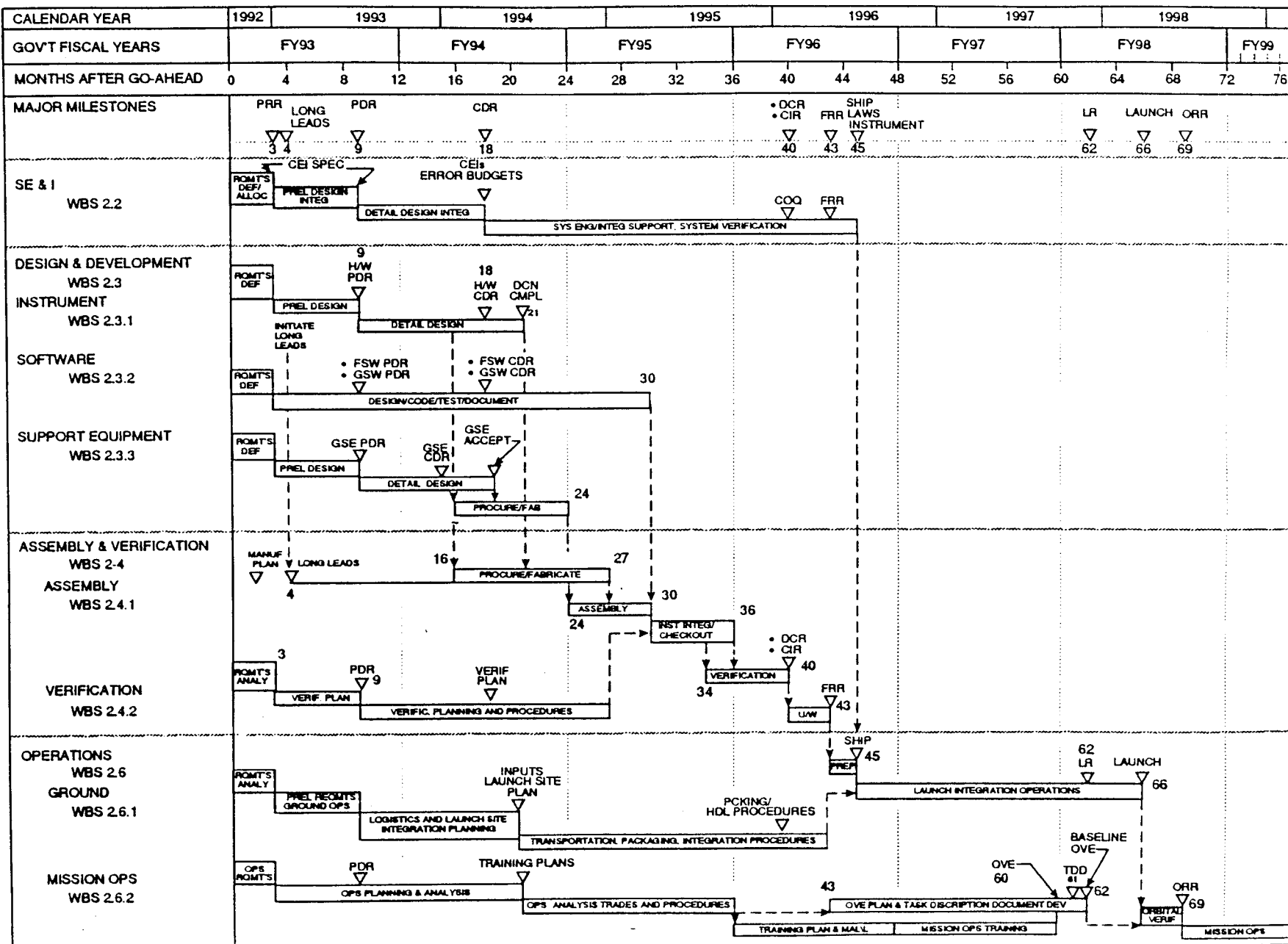


Figure 46. Preliminary LAWS Master Schedule for JP0P Phase C/D

- I. DESIGN AND DEVELOPMENT
  - 1. LASER SUBSYSTEM, WBS 2.4.3.1.1
    - TRANSMITTER
    - OTHER
  - 2. OPTICAL SUBSYSTEM, WBS 2.4.3.1.2
    - TELESCOPE
    - BEAM SCANNER
    - INTERFEROMETER
    - LOCAL OSCILLATOR ASSEMBLY
    - LOCAL OPTICAL BENCH
    - OTHER
  - 3. CMD, COMM, CTRL, WBS 2.4.3.1.3
    - FLIGHT COMPUTER
    - OTHER
  - 4. RECEIVER/PROCESSOR SUBSYSTEM, WBS 2.4.3.1.4
    - IR DETECTOR ASSEMBLY
    - CRYOGENIC ASSEMBLY
    - RECEIVER ELECTRONICS
    - OTHER
  - 5. ELECTRICAL POWER SUBSTATION, WBS 2.4.3.1.5
    - POWER DIST NETWORK
    - POWER COND ELECTRONICS
    - OTHER
- 6. MECHANICAL SUPPORT SUBSYSTEM, WBS 2.4.3.1.6
  - INSTRUMENT OPTICAL BENCH
  - THERMAL CONTROL SYSTEM
  - OTHER
- 7. SPARES, WBS 2.4.3.4
- 8. SYSTEM SUPPORT EQUIPMENT, WBS 2.4.3.2
  - a. GROUND SUPPORT EQUIPMENT
    - MECHANICAL
    - ELECTRICAL
  - b. AIRBORNE SUPPORT EQUIPMENT
- 9. SYSTEM DESIGN, INTEGRATION & TEST, WBS 2.1 - 2.8
  - a. SYSTEM ENGINEERING
  - b. INSTRUMENT ENGINEERING
  - c. ASSEMBLY AND VERIFICATION
  - d. PRODUCT ASSURANCE AND SAFETY
  - e. OPERATIONS/LOGISTICS
  - f. PROJECT MANAGEMENT
  - g. SOFTWARE DEVELOPMENT
  - FLIGHT, SIMULATION, GROUND
- II. LAUNCH INTEGRATION, WBS 2.6.1.3
- III. PROTOTYPE MISSION OPERATIONS, WBS 2.6.2.3

Figure 47. LAWS Instrument Cost Elements

Cost Estimating Relationships and Cost Factors. Design at the system level, project management at the system level, system integration, and test for operation were accounted for by the program wrap Cost Estimating Relationships (CERs) mentioned above. These CERs were used to compute the following cost elements:

1. System engineering
  2. Instrument engineering
  3. Assembly and verification
  4. Product assurance
  5. Operations/logistics
  6. Project management
  7. Spares
  8. GSE.

Travel is included in each CER. The assembly and verification CER includes utilization of privately owned test facilities. It does not include the construction of any LAWS unique facilities. Current analysis does not indicate a requirement for LAWS unique facilities. The operations/logistics CER includes shipping.

LAWS program wrap CERs were computed as a function of the total subsystem costs. Launch integration and mission operations support are estimated values at this stage of the analysis. Spares were estimated as a function of the total subsystem.

RCA-PRICE default values were used for all "GLOBALS" in the model. The year of economics was input as 1989. The year of technology was assumed to be 1992. For purposes of the current analysis, the RCA-PRICE model computed the development schedule.

### 5.3 SUMMARY COST PRESENTATIONS

This section summarizes the LAWS Phase I cost modeling and analysis activities. Figure 48 presents the cost estimates for both the JPOP and the Space Station instruments. Subsystem costs were estimated at the component/assembly level and "rolled up" to the appropriate subsystem level. The same procedure was used for the system integration wraps used to generate the cost elements for WBS Elements 2.1 through 2.7. This procedure is consistent with definitions currently available and the uncertainties that exist in the cost estimates.

The expected value for the JPOP instrument is \$168.1M. With uncertainties considered, the cost estimate is expected to be between \$155M and \$181M, which is within the 15 to 20 percent estimating accuracy normally accepted for this type of estimate. The primary contributions to the uncertainties are weight, manufacturing complexities, and the program factor representative of unmanned space vehicles.

The uncertainties were estimated by considering an expected error in the above parameters and then computing the associated cost impact. These uncertainties represent a contingency to account for unknowns in the program and in hardware and software definitions. The uncertainty contributions were assumed to behave as a normal error distribution.

WBS ELEMENT	COST ELEMENT	JPOP INSTRUMENT		SPACE STATION		SPACE STATION & JPOP TOTAL \$M
		SUBTOTAL \$M	TOTAL \$M	SUBTOTAL \$M	TOTAL \$M	
2.4.3.1.1	LASER SUBSYSTEM	36.5		19.6		
2.4.3.1.2	OPTICAL SUBSYSTEM	27.8		8.8		
2.4.3.1.3	CMD. COMM. CTRL	2.8		.9		
2.4.3.1.4	RECEIVER/PROCESSOR	3.8		2.7		
2.4.3.1.5	ELECT PWR DIST	3.7		1.0		
2.4.3.1.6	MECH STRUCTURE	10.8	85.4	2.3	35.3	120.7
2.4.3.4	SPARES	17.1		3.5		
2.4.3.2	GSE	6.8	23.9	0.7	4.2	28.1
see note 2.3.2	SYS DES, INT & TEST SOFTWARE	27.9 3.0	30.9	5.9 1.0	6.9	37.8
2.6.1.3	LAUNCH INTEGRATION	3.0		1.5		
2.6.2.3	OPERATION & SUPPORT	3.0	6.0	3.0	4.5	10.5
2.8	ORBITAL SERVICING			14.8	14.8	14.8
	FEE/BURDENS	21.9	21.9	9.8	9.8	31.7
2.0	TOTAL PROJECT	EXPECTED: 168.1 LOW: 154.9 HIGH: 181.4			75.5	243.6

NOTE: includes 2.1 - 2.7

**Figure 48. JPOP and Space Station Development Cost**

#### 5.4 FUNDING PROFILES AND EXPENDITURES DATA

Figure 49 displays the funding curve and the expenditures for the activities associated with the LAWS Instrument development for the JPOP. Funding profiles are based on 1989 dollars. The profiles represent the time phasing of the cost model results presented in Figure 48. The top profile of Figure 49 depicts the cumulative project cost. The bottom profile represents the project wrap activities and includes labor, travel, launch integration, and mission operations support activities and other direct costs. These are Items II and III from Figure 47. For Phase I analysis, it has been assumed that common PDRs and CDRs will be held for the flight hardware and software and for the GSE hardware and software.

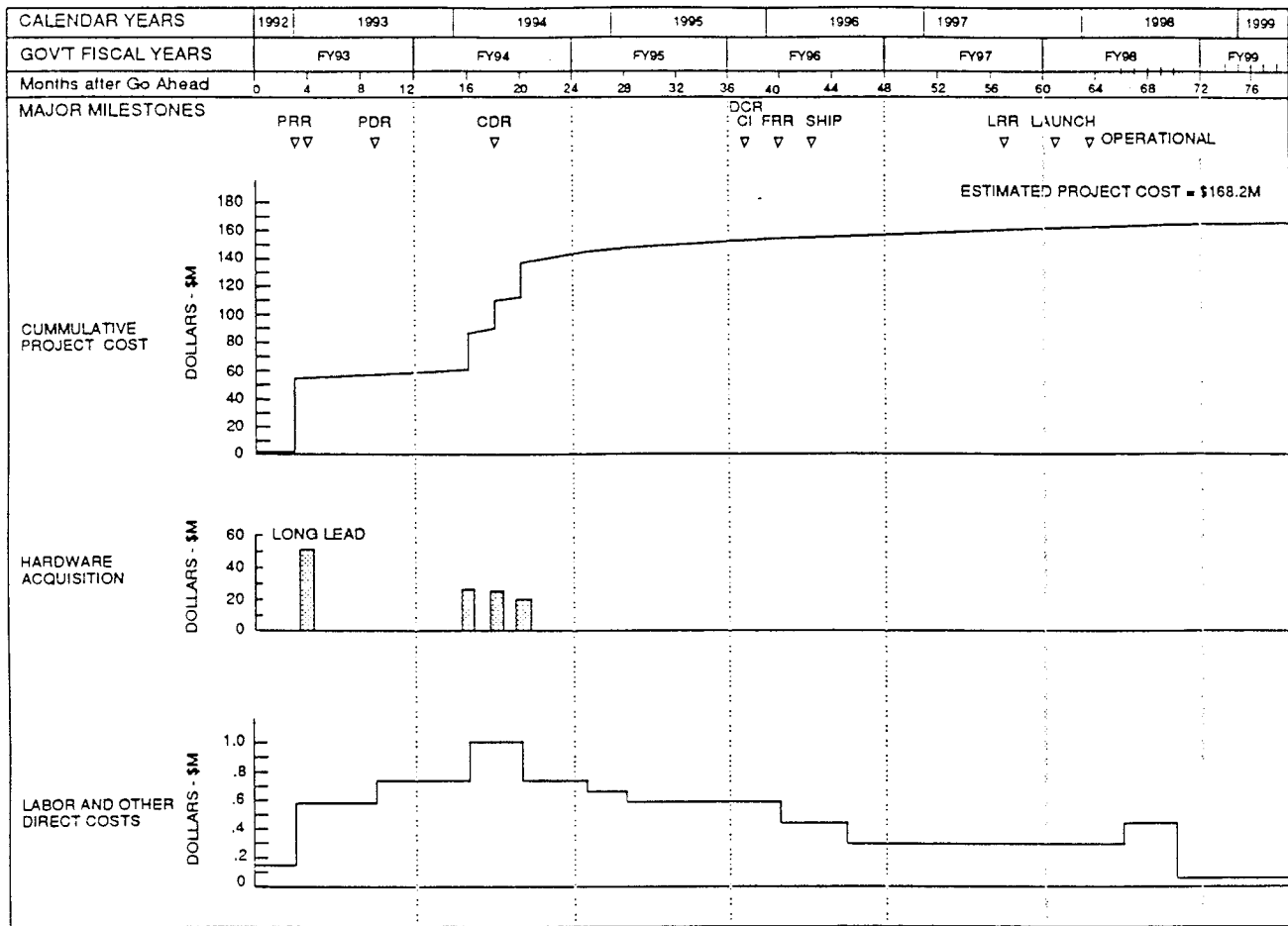


Figure 49. Projected Funding Profiles for LAWS Phase C/D to Develop the JPOP Configuration

The middle profile is presented in bar chart format because it represents the commitment to procure the hardware items. Phase I analysis indicates that the laser and telescope are long lead items. The commitment for these is shown at month four. The second commitment of hardware acquisition funds is expected to occur shortly before the flight hardware CDR, as drawings and specifications are released for the procurement and fabrication process. The third and fourth commitments of hardware acquisition occur as the final drawings are released after CDR. It should be remembered from previous discussions that the assumption has been made for Phase I analysis purposes that all subsystems are procured from outside sources. In reality there are some prime contractor labor and other direct costs associated with the subsystem cost allocations. These will be redistributed to proper WBS cost elements and the funding profiles adjusted once the subsystem components are defined.